Neutron Stars and Black Holes

Kostas Kokkotas
University of Tübingen & Thessaloniki

An extreme challenge

Neutron star modelling involves the very extremes of physics:

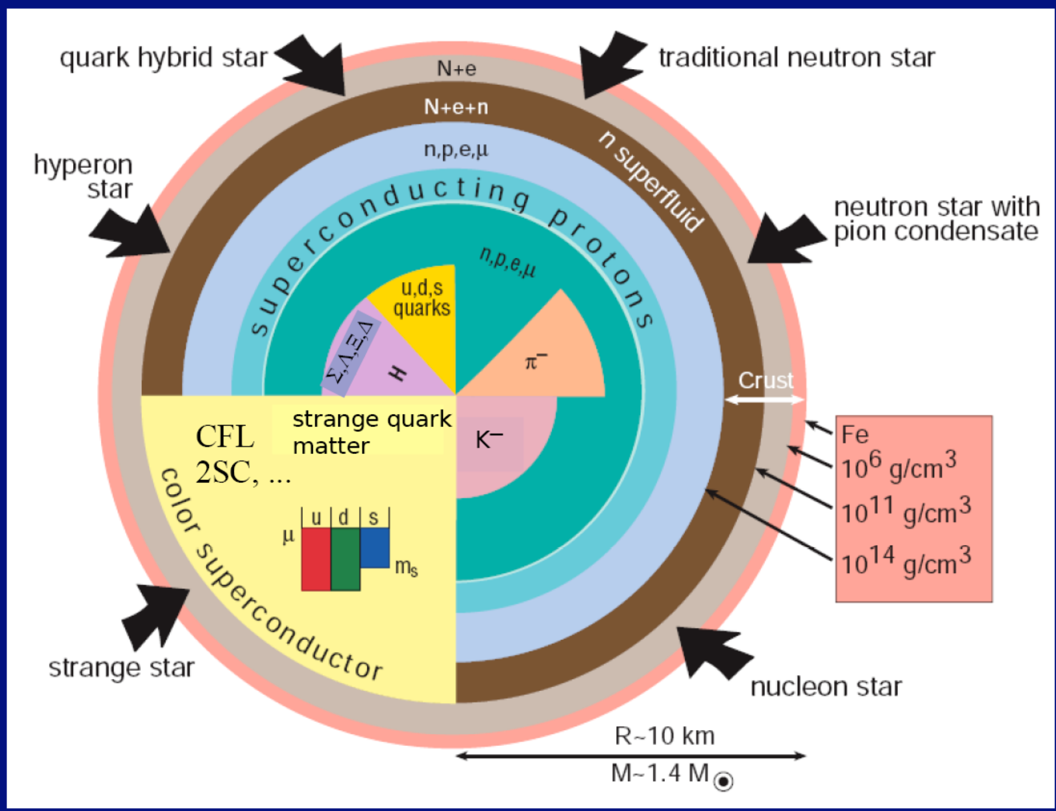

F. Weber, Prog. Part. Nucl. Phys. 54 (2005) 193-288

1. rapid (differential) rotation
2. general relativity
3. superfluidity
4. strong magnetic fields
5. crust-core interface
   Ekman/Alfven layer
6. exotic nuclear physics
   strange quarks, hyperons
7. …

Can GW, x-ray, γ-ray observations constrain the theoretical models?

Why stellar oscillations & instabilities?

- Understand the internal structure of astronomical objects
- Unique research field for both Newtonian and Relativistic hydrodynamics
- Oscillations & Instabilities are related to the various evolutionary phases of the stars
- A field were perturbation and non-linear physics meet.
- One of the best sources of gravitational waves

Equilibrium & Stability

- Fluid Equations

$$\frac{\partial \rho}{\partial t} + \nabla \cdot \left(\rho \vec{v} \right) = 0$$

$$\frac{d\vec{v}}{dt} = -\frac{1}{\rho} \nabla p - \nabla \Phi$$

$$\nabla^2 \Phi = 4\pi G \rho$$

$$\frac{d}{dt} = \frac{\partial}{\partial t} + \vec{v} \cdot \nabla$$

- Hydrostatic Equilibrium

$$\vec{v} = 0 \;\Rightarrow\; \nabla p = -\rho \nabla \Phi$$

- Equilibrium from an extremum of the Energy

$$\delta\rho + \nabla\left(\rho \vec{\xi}\right) = 0$$

$$-\sigma^2 \vec{\xi} + \frac{1}{\rho} \nabla\left(\delta p\right) + \nabla\left(\delta \Phi\right) + \frac{\delta \rho}{\rho} \nabla \Phi = 0$$

$$\frac{1}{r^2} \partial_r \left[r^2 \partial_r \left(\delta \Phi \right) \right] + \nabla_\perp^2 \left(\delta \Phi \right) = 4\pi G \delta \rho$$

$$\frac{\delta \rho}{\rho} = \frac{1}{\Gamma_1} \frac{\delta p}{p} - A\xi$$

Small Perturbations about Equilibrium

USEFUL because they enable us:

1. **To calculate the frequencies of normal modes of oscillation**
2. **To study the stability of the equilibrium state**

The dynamics is governed by the perturbed Euler equation

$$\Delta\left(\frac{dv^i}{dt} + \frac{1}{\rho}\nabla_i p + \nabla_i \Phi\right) = 0$$

$$\Delta v^i = \frac{d\xi^i}{dt}$$

$$\rho\frac{d^2\xi^i}{dt^2} - \frac{\Delta\rho}{\rho}\nabla_i p + \nabla_i \Delta p + \rho\nabla_i \Delta\Phi = 0$$

$$\rho\partial_t^2\xi^i = \mathrm{L}^i{}_j\xi^j \Rightarrow -\omega^2\rho\xi^i = \mathrm{L}^i{}_j\xi^j$$

$$\xi \sim \xi(r)\cdot e^{i\omega t}$$

Example : Radial Oscillations

- Perturbation Equation

$$-\omega^2 \rho \xi = \frac{d}{dr}\left(\Gamma_1 p \frac{1}{r^2}\frac{d}{dr}\left(r^2 \xi\right)\right) - \frac{4}{r}\frac{dp}{dr}\xi$$

$$\Gamma_1 = \left(\frac{\partial \ln p}{\partial \ln \rho}\right)_s$$

- Boundary Conditions

$$\xi(r=0) = 0$$

$$\Delta P(r=R) = 0$$

- Sturm-Liouville
  - Real e-values ω^2
  - Infinite discrete sequence of real e-values $\omega_0^2 < \omega_1^2 < \omega_2^2 \ldots$
  - The e-function ξ_0 corresponding to ω_0^2 has no nodes in the interval $0<r<R$ while ξ_n has n nodes.

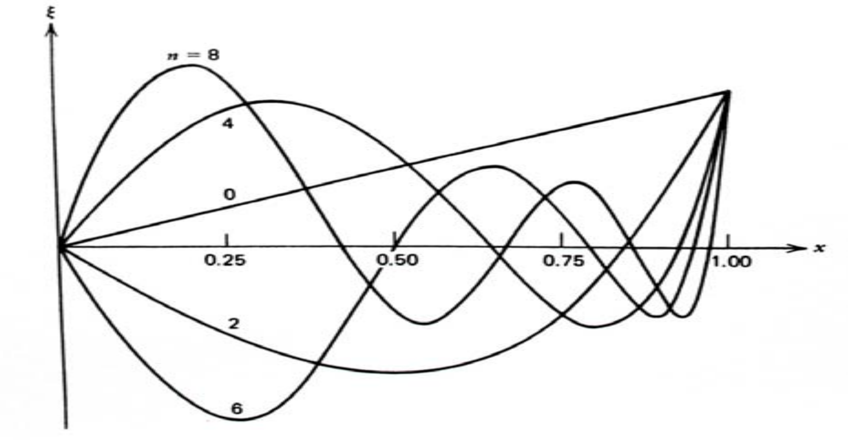

  - Homogeneous star

$$\omega^2 = \frac{2}{3}\pi G \rho \left[\Gamma_1\left(n^2 + 5n + 6\right) - 8\right], \quad n = 0, 2, 4, \ldots \text{Unstable if: } \Gamma_1 < 4/3$$

Stability Criteria

- Small deviations from equilibrium

$$E = E_0 + \delta E + \delta^2 E$$
$$\delta^2 E \equiv E_2 = T_2 + V_2 = \delta^2 T + \delta^2 \left(U + W\right)$$

- Instability: unbounded growth of a small initial perturbation $(\xi_i, \partial_t \xi^i)$, or unbounded growth of the kinetic energy of the perturbation T_2.
- Stability: the necessary & sufficient condition is that the potential energy of the perturbation V_2 be positive definite for all initial data.

$$V_2 \geq 0 \Leftrightarrow \text{stability}$$

- Stability via normal mode analysis

$$\omega^2 = \frac{V_2}{I} = -\frac{\int \rho\left(\partial_t \xi^i\right)^2 d^3x}{\int \rho \xi^i \xi^i d^3x}$$

$$V_2 \geq 0 \Leftrightarrow \omega^2 \geq 0 \Leftrightarrow \text{stability}$$

- Radial perturbations

$$\omega^2 = \frac{\int_0^R \left[\Gamma_1 p \frac{1}{r^2}\left(\frac{d}{dr}\left(r^2 \xi\right)\right)^2 + 4\frac{dp}{dr}\xi^2\right] dr}{\int_0^R \rho \xi^2 r^2 dr} \propto 3\overline{\Gamma}_1 - 4$$

- Turning-Points

$$\frac{\partial^2 E}{\partial {\rho_c}^2} \approx \frac{dM}{d\rho_c} \propto \Gamma - \frac{4}{3} - \kappa \frac{GM}{Rc^2}$$

Mass-Radius diagram

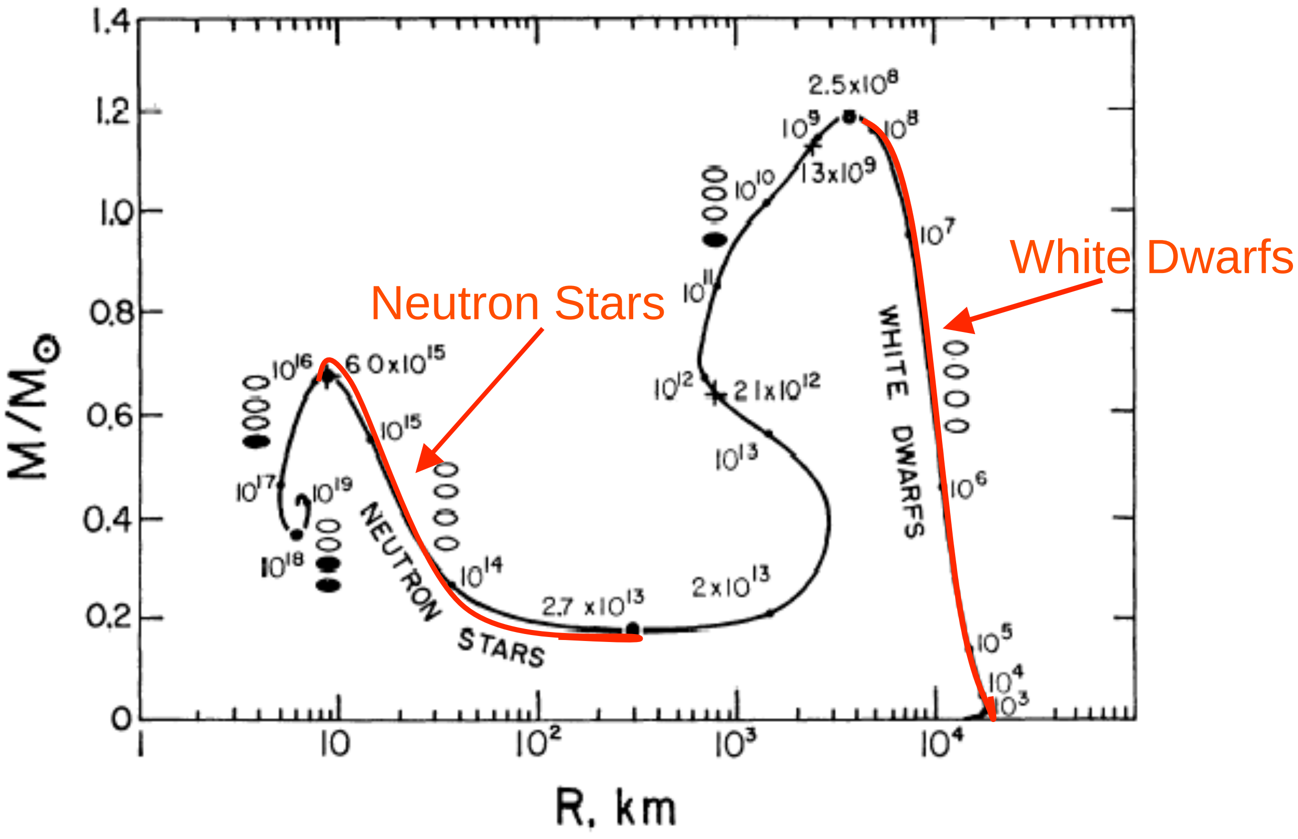

FIG. 2.—Mass-radius curve for Harrison-Wakano-Wheeler configurations. The curve is parameterized by central density measured in grams per cubic centimeter. At each peak and valley in the curve (*large dots*) one normal radial mode changes stability. Between peaks and valleys each unstable normal mode is represented by a blackened oval, while the stable modes are represented by open ovals. Configurations between the first peak and the first cross ($2.5 \times 10^8 < \rho_c < 1.3 \times 10^9$) are metastable, "molasses-like" white dwarfs with lifetimes $\gtrsim 10^{10}$ years; configurations between the second cross and the first valley ($2.1 \times 10^{12} < \rho_c < 2.7 \times 10^{13}$) are metastable neutron stars with lifetimes $\gtrsim 100$ days.

Mass vs Radius Diagram

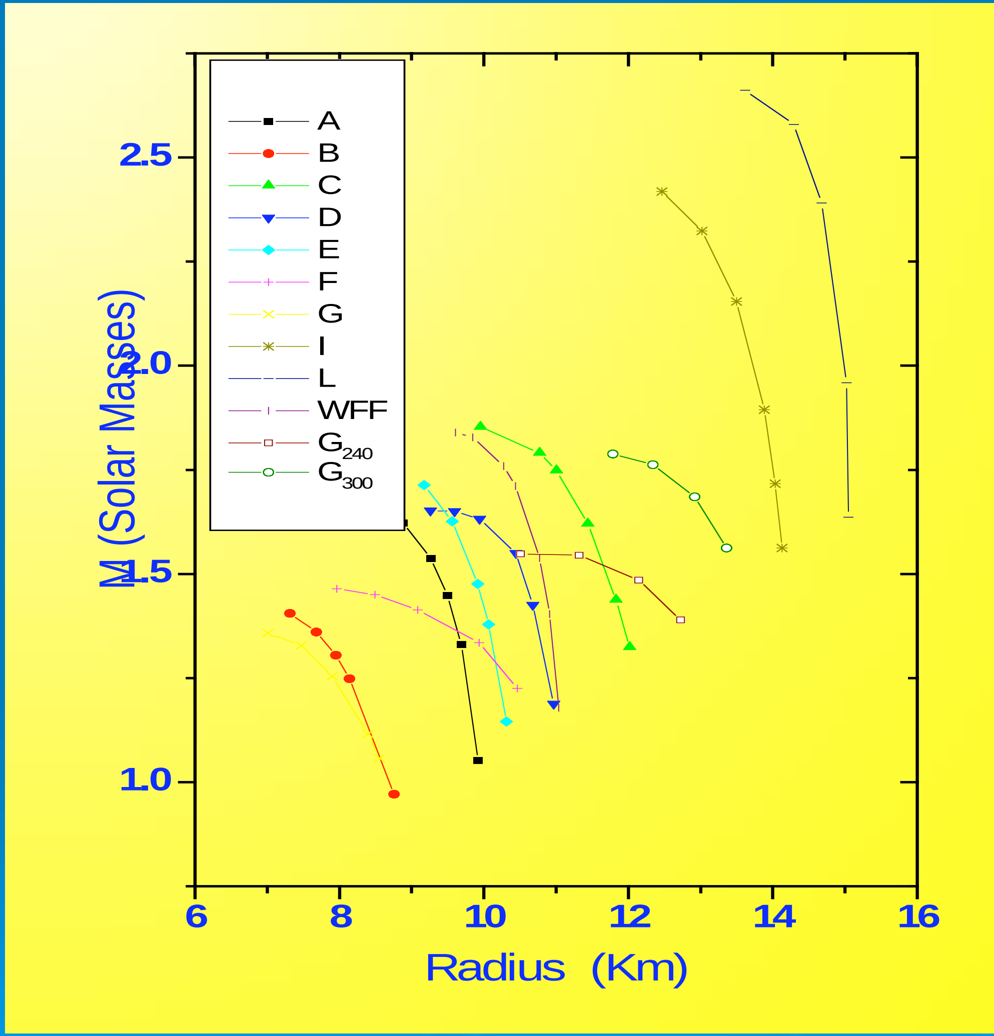

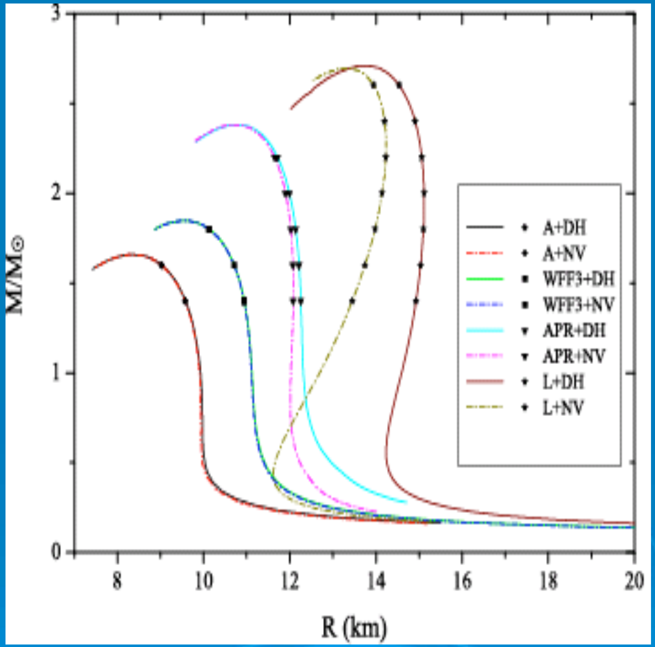

Stability of non-radial perturbations

- Equations describing non-radial oscillations…
- **Schwarzschild discriminant**: is related to the convective instability in a star
- If A>0 (or $\Gamma_1 > \Gamma$) somewhere inside the star the matter will be unstable to convective motions i.e. g-modes become unstable.
- A is proportional to the frequency *N* at which a fluid element may oscillate around its equilibrium position under the influence of gravity and pressure gradients. It is called a Brunt-Väisälä frequency

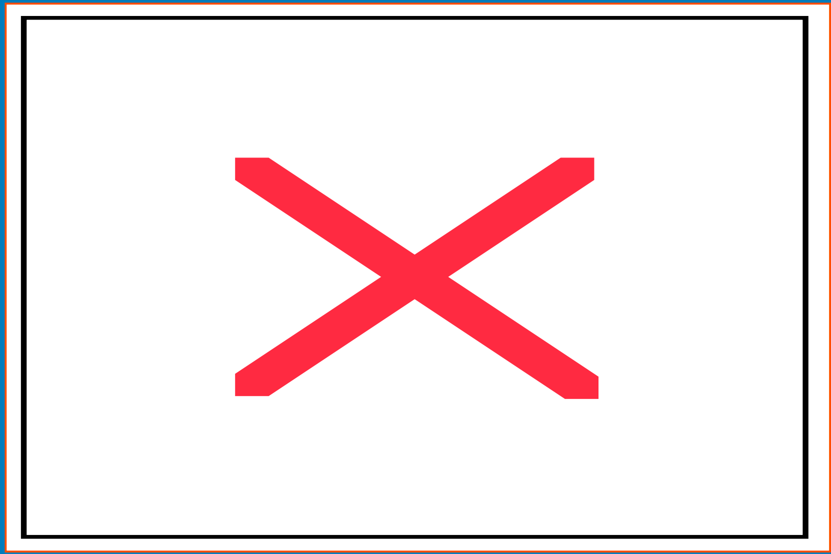

$$A \equiv \frac{d\ln\rho}{dr} - \frac{1}{\Gamma_1}\frac{d\ln p}{dr} = \left(\frac{1}{\Gamma} - \frac{1}{\Gamma_1}\right)\frac{d\ln\rho}{dr}$$

$$N^2 \equiv -Ag, \quad g \equiv \frac{GM(r)}{r^2}$$

Rotating Configurations
(Maclaurin Spheroids)

Maclaurin spheroids: uniformly rotating & uniform density ellipsoids

- A uniformly rotating spheroid in hydrostatic equilibrium satisfies:

$$\frac{d\vec{v}}{dt} = -\frac{1}{\rho}\nabla p - \nabla\Phi$$

$$\vec{v} = \vec{\Omega}\times\vec{r} \Rightarrow \frac{d\vec{v}}{dt} = \vec{\Omega}\times\left(\vec{\Omega}\times\vec{r}\right)$$

Angular velocity: $\Omega = 2\pi G\rho\, f_1(e)$

Mass: $M = \frac{4}{3}\pi\rho a^3\left(1-e^2\right)^{1/2}$

Moment of Inertia: $I = \frac{2}{3}Ma^2$

Angular Momentum: $J = I\cdot\Omega$

Kinetic Energy: $T = \frac{1}{2}I\cdot\Omega^2$

Grav. Poten. Energy: $W = G\rho^2 a^5 f_2(e)$

- A useful parameter:

$$\beta = \frac{T}{|W|} = \frac{3}{2e^2}\left(1-\frac{e(1-e^2)^{1/2}}{\sin^{-1}e}\right)-1$$

- Stability of Maclaurin spheroids (nonradial oscillations)
  - Secularly unstable

    $e > 0.953 \quad \text{or} \quad \beta > 0.274$
  - Dynamically unstable

    $e > 0.813 \quad \text{or} \quad \beta > 0.138$

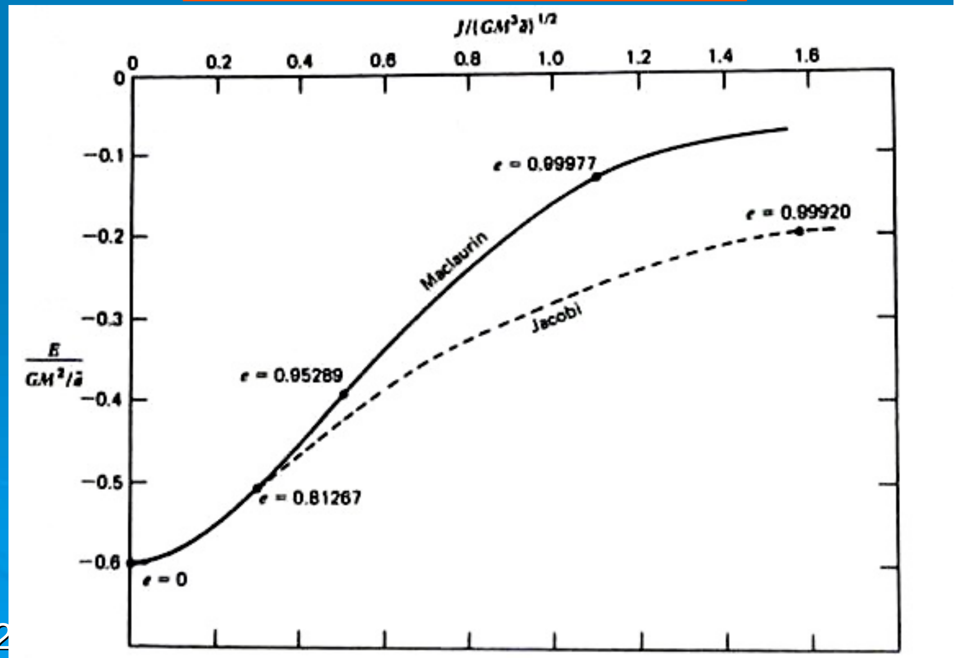

Secular Instability

Maclaurin shds are unstable beyond the bifurcation point =>Jacobi/Dedekind elds.

Jacobi ellipsoids

- uniformly rotating, with ellipsoidal surfaces. They have no vorticity ($\zeta=0$) when viewed from a rotating frame, in which the figure appears stationary.
- For a given *angular momentum, mass and volume* has lower energy than the corresponding Maclaurin

Dedekind ellipsoids

- They have a stationary triaxial shape in the inertial frame ($\Omega=0$). The shape is supported by internal motions of uniform vorticity
- The Dedekind ellipsoid with the same *mass* and *circulation* as the corresponding Maclaurin has lower angular momentum

- TWO alternative states with lower energy/ang.momentum for $\beta>0.14$. Transition is possible if a dissipative term is added (since the dynamical eqns conserve energy/circulation).
- An instability due to the presence of dissipation is called **secular instability**
- **Viscosity driven** instability drives the system towards the Jacobi sequence, because dissipates energy while preserves angular momentum.
- **GWs**, radiates angular momentum while conserves internal circulation. It is driving the system towards the Dedekind sequence (which don't radiate gravitationally)

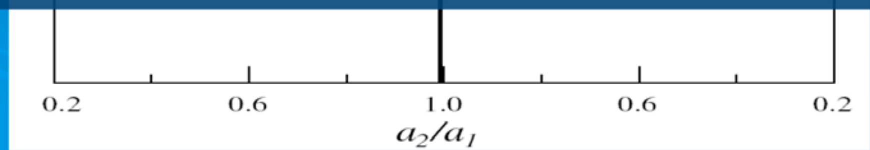

Maximum Rotation

- For fast rotating stars *β=T/|W|* is limited by the condition of no mass shedding at the equator.
- Centrally condensed objects in uniform rotation might lose mass before rotating fast enough to encounter the secular/dynamical instabilities
- Still, differentially rotating objects allow $0 \leq \beta \leq 0.5$

Break up velocity (spherical star)

$$v^2 = \Omega^2 R^2 = \frac{GM}{R}$$

•A *n=3* polytrope will break up for *T/|W|=0.025*

•A *n->0* (incompressible fluid) will break up for *T/|W|=1/3*

Break up velocity (realistic):

$$v^2 = \Omega^2 R^2 = \left(\frac{2}{3}\right)^3 \frac{GM}{R}$$

•A n=3 polytrope will break up for T/|W|=0.0075

•Mass shedding occurs before the bifurcation point for all polytropes with n>0.88

$$\Omega_{\text{Kepler}} \sim \sqrt{\frac{GM}{R^3}}$$

A relativistic star (no-rotation)

- The metric $$ds^2 = -e^{\nu(r)}dt^2 + e^{\lambda(r)}dr^2 + r^2(d\theta^2 + \sin^2\theta d\varphi^2)$$
- Energy-momentum tensor $$T_{\mu\nu} = (\rho + p)u_\mu u_\nu + pg_{\mu\nu}$$
- Energy-momentum conservation +Einstein eqns $$T^{\mu\nu}{}_{;\nu} = 0, \quad R_{\mu\nu} = k\left(T_{\mu\nu} - \frac{1}{2}g_{\mu\nu}T\right)$$
- TOV equations:
$$\frac{dm}{dr} = 4\pi\rho r^2$$
$$\frac{d\nu}{dr} = 2\frac{e^\lambda}{r^2}(m + 4\pi pr^3)$$
$$\frac{dp}{dr} = -\frac{\rho + p}{2}\frac{d\nu}{dr}$$
$$e^{-\lambda} = 1 - \frac{2m(r)}{r}$$
- + EoS ***p=p(ρ)***
- *Maximum "compaction" of a uniform density star:*

$$\frac{2M}{R} < \frac{8}{9}$$

Stellar Surface R at: $p(r) = 0$

normalization of $\nu(r)$: $e^{\nu(R)} = 1 - \frac{2M}{R}$

Rotating Relativistic Stars

- Spacetime

$$ds^2 = -e^{\nu(r,\theta)}dt^2 + e^{\mu(r,\theta)}(dr^2 + r^2 d\theta^2) + e^{\psi(r,\theta)} r^2 \sin^2\theta (d\varphi - \omega(r,\theta)dt)^2$$

$$ds^2 = -e^{\nu(r)}dt^2 + e^{\lambda(r)}dr^2 + r^2(d\theta^2 + \sin^2\theta d\varphi^2) - 2\omega(r) r^2 \sin^2\theta dt d\varphi$$

- Energy-momentum tensor

$$T_{\mu\nu} = (\rho + p)u_\mu u_\nu + p g_{\mu\nu}$$

- Energy-momentum conservation + Einstein equations

$$\nabla_\mu T^{\mu\nu} = 0$$

$$R_{\mu\nu} = k\left(T_{\mu\nu} - \frac{1}{2} g_{\mu\nu} T\right)$$

- EoS ***p=p(ρ,s,…)***

Slow rotation is not too bad!
P=1.5ms, R=10km, M=1.4$M_\odot$

$$\varepsilon = \Omega / \Omega_{\text{Kepler}} \approx 0.3$$

Stellar Perturbation Theory

Take variations of Einstein's eqns and the energy-momentum conservation

$$\delta \begin{pmatrix} \nabla_\mu T^{\mu\nu} = 0 \\ R_{\mu\nu} = k\left(T_{\mu\nu} - \frac{1}{2} g_{\mu\nu} T\right) \end{pmatrix}$$

Assume small variation in pressure, density, fluid velocities and in the metric.

$$\delta P \sim \delta P(t,r) \cdot Y_m^l(\theta,\varphi), \;\; \delta\rho \sim \delta\rho(t,r) \cdot Y_m^l(\theta,\varphi)$$

$$\tilde{g}_{\mu\nu} = g_{\mu\nu} + h_{\mu\nu}(t,r,\theta,\varphi), \; h_{\mu\nu} \sim h_{\mu\nu}(t,r) \cdot Y_m^l(\theta,\varphi)$$

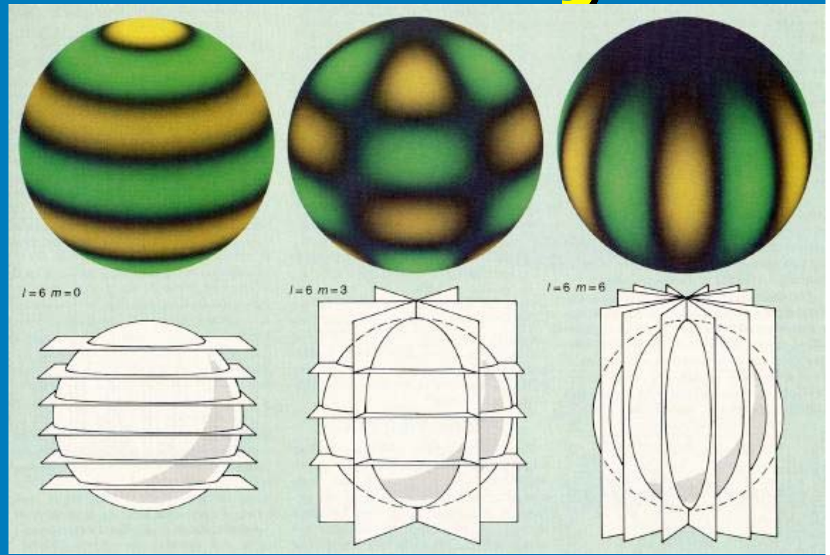

For a spherical star every l correspond $2l+1$ modes i.e. degeneracy with respect to m.

- Stellar model: fluid core, solid crust & thin surface ocean
- Broad diversity of oscillation modes
- Frequencies: 0.1Hz - 10kHz
- Two main classes: Spheroidal & Toroidal

Neutron Star "ringing"

- **p-modes:** main restoring force is the pressure **(f-mode)** (can become unstable) $\omega^2 \sim M/R^3$ *(>1.5 kHz)*
- **Inertial modes (r-modes)** main restoring force is the Coriolis force (can become unstable) $\omega \sim \Omega$
- **Torsional modes** (t-modes) $\omega^2 \sim l(l+1)u_s/R$ *(>20 Hz)* shear deformations, divergence-free, with no-radial components. Restoring force, the weak Coulomb force of the crystal ions. (can become unstable)
- **w-modes:** pure space-time modes (only in GR) (can become unstable) $\omega \sim 1/R$ *(>5kHz)*

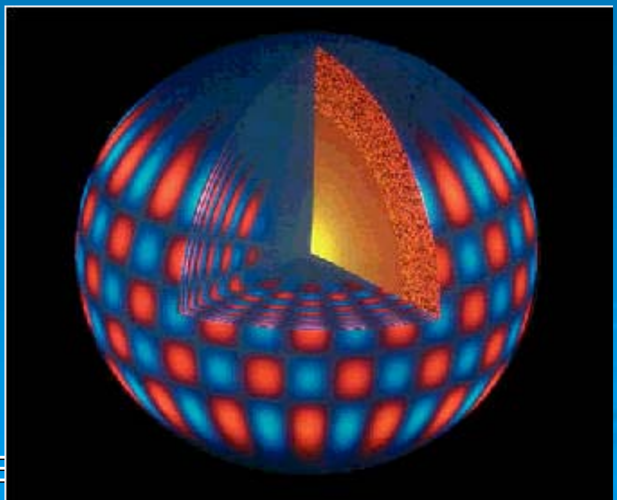

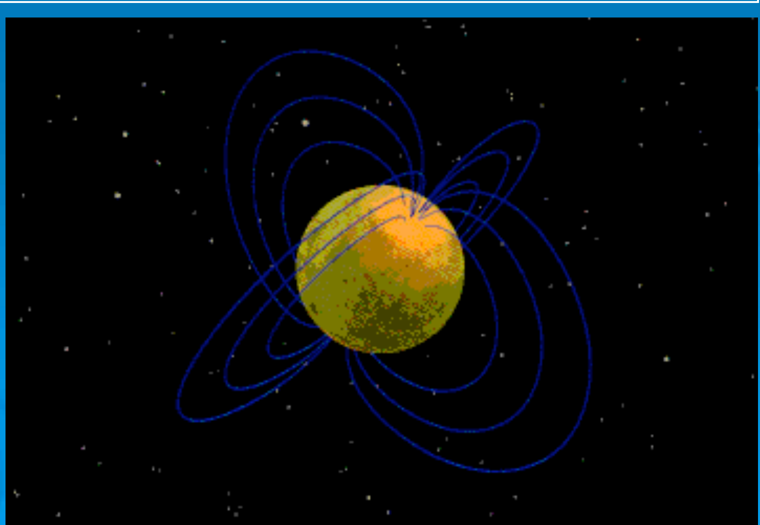

Grav. Wave Asteroseismology

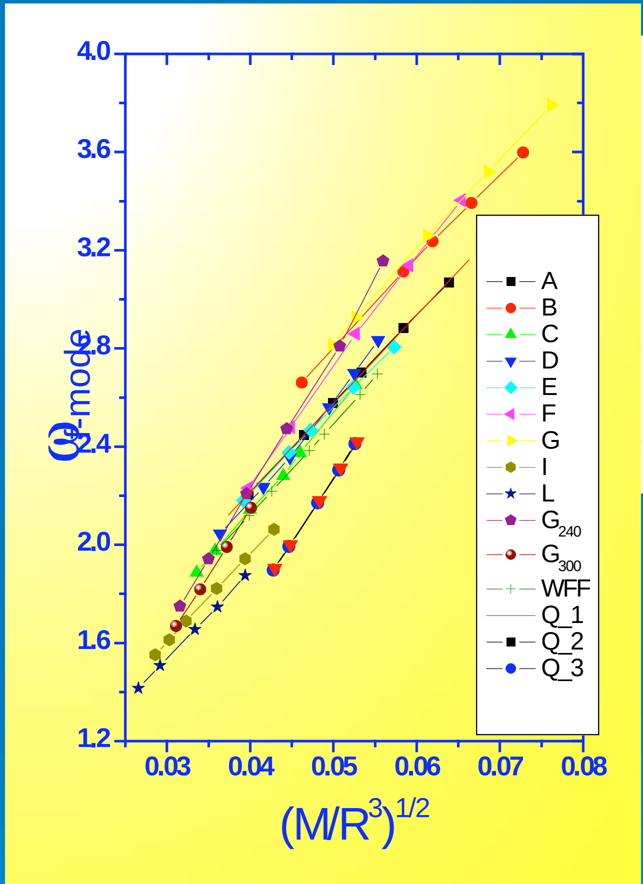

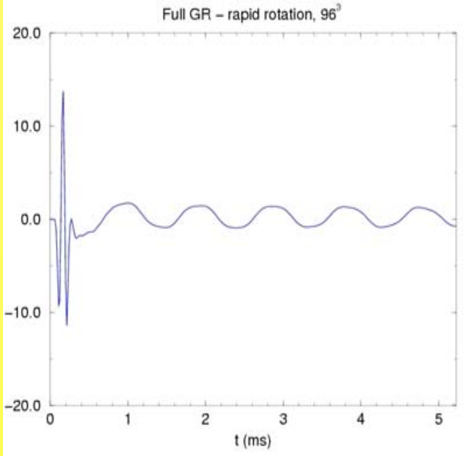

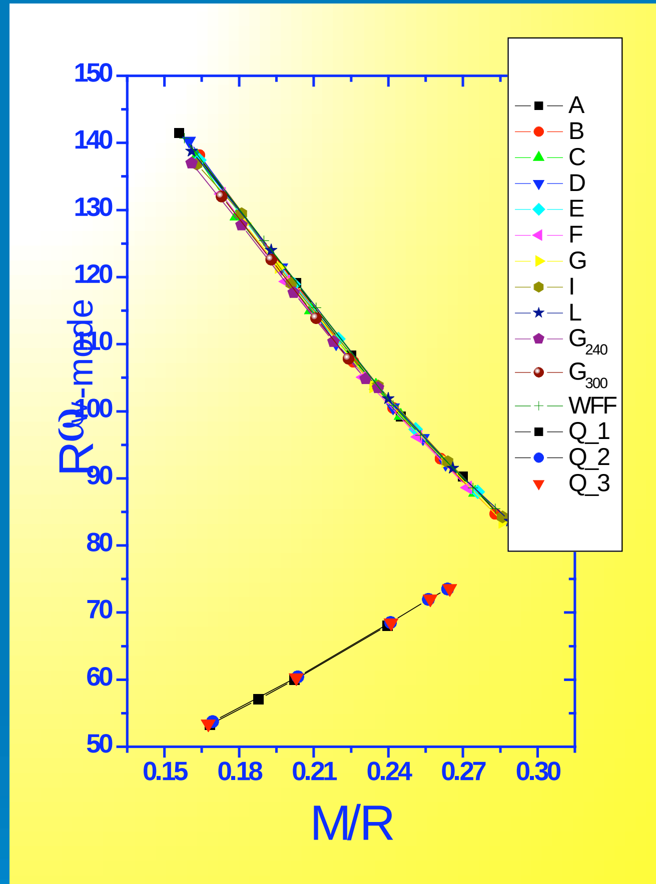

$$\omega_f(kHz) \approx 0.8 + 1.6\left(\frac{M_{1.4}}{R_{10}^{\ 3}}\right)^{1/2} + \delta_f m \frac{\Omega}{\Omega_K}$$

$$\omega_w(kHz) \approx \frac{1}{R_{10}}\left[21 - 9\frac{M_{1.4}}{R_{10}}\right] + \delta_w m \frac{\Omega}{\Omega_K}$$

Andersson + KK (96,98,01)

Effects of Rotation

- Frame dragging
- Quadrupole deformation
- The degeneracy in m is removed and the nonrotating mode of index ℓ is split into 2ℓ+1 different (ℓ,m) modes
- Shifting of the frequencies and damping times
- Rotational instabilities
- Coupling of polar ℓ-term to an axial ℓ±1 term and v-v

$$
\begin{aligned}
P_{l,m} + \mathrm{i}m\Omega P_{l,m} + \Omega \mathcal{L}_i^{\pm 1} A_{l,m} + \Omega^2 \mathcal{L}_i^{\pm 2} P_{l,m} &= 0, \\
A_{l,m} + \mathrm{i}m\Omega A_{l,m} + \Omega \mathcal{L}_i^{\pm 1} P_{l,m} + \Omega^2 \mathcal{L}_i^{\pm 2} A_{l,m} &= 0,
\end{aligned}
$$

In a sequence of rotating stellar models, a QNM of index ℓ is defined as the mode which in the limit Ω->0 reduces to the QNM of the same index ℓ.

Stability of Rotating Stars

Non-Axisymmetric Perturbations

A general criterion is:

$$\beta = \frac{T}{W}$$

T : rot. kinetic energy
W : grav. binding energy

Dynamical Instabilities

- Driven by hydrodynamical forces (bar-mode instability)
- Develop at a time scale of about one rotation period $\sim (G\rho)^{-1/2}$

$$\beta \geq 0.27$$

Secular Instabilities

- **Driven by dissipative forces (*viscosity*, *gravitational radiation*)**
- **Develop at a time scale of several rotation periods.**
- **Viscosity driven instability causes a Maclaurin spheroid to evolve into a non-axisymmetric Jacobi ellipsoid.**
- **Gravitational radiation driven instability causes a Maclaurin spheroid to evolve into a stationary but non-axisymmetric Dedekind ellipsoid.**

Chandrasekhar-Friedman-Schutz (CFS)

$$\beta \geq 0.14$$

GR and/or differential rotation suggest considerably lower β for the onset of the instabilities

The pattern speed

- The pattern speed σ of a mode is:

$$\frac{d\varphi}{dt} = -\frac{\omega}{m} = \sigma$$

- If a star rotates very fast, a backward moving mode, might change to move forward, *according to an inertial observer.*

$$\omega_{\text{inert}} = \omega_{\text{rot}} + m\Omega$$
$$\sigma_{\text{inert}} = \sigma_{\text{rot}} + \Omega$$

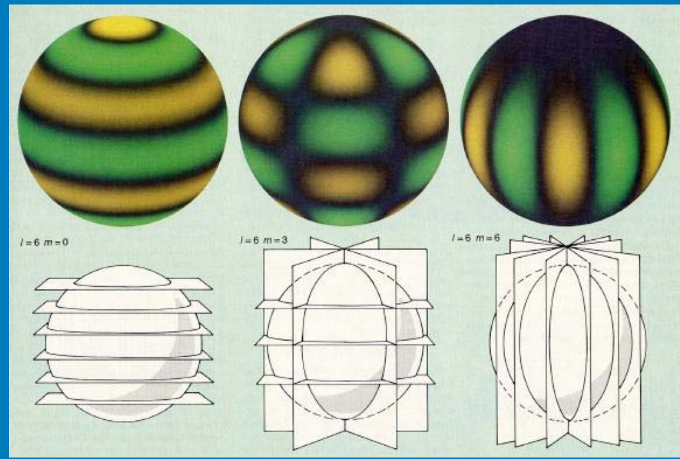

The CFS instability

Chandrasekhar 1969: Gravitational waves lead to a secular instability
Friedman & Schutz 1978: The instability is generic, modes with sufficiently large *m* are unstable.

A **neutral mode** of oscillation signals the onset of CFS instability.

- Radiation drives a mode unstable if the mode pattern moves backwards according to an observer on the star *(J_{rot}<0)*, but forwards according to someone far away *(J_{rot}>0)*.
- They radiate positive angular momentum, thus in the rotating frame the angular momentum of the mode increases leading to an increase in mode's amplitude.

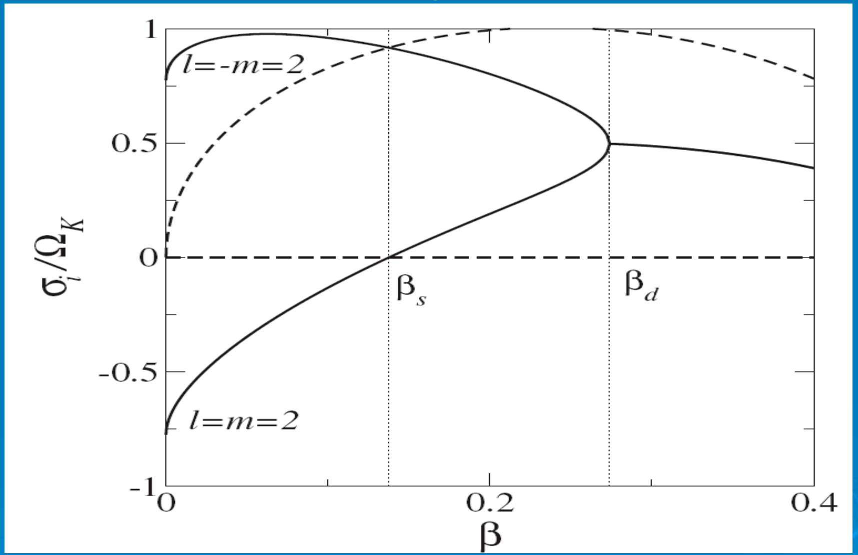

$$\frac{\omega_{\text{in}}}{m} = -\frac{\omega_{\text{rot}}}{m} + \Omega$$

f-mode

- f-mode is the fundamental pressure mode of the star
- It corresponds to polar perturbations
- Frequency for uniform density stars

$$\omega^2 = \frac{2l(l-1)}{2l+1}\frac{GM}{R^3}$$

growth time(if unstable)

$$t_{GW} \approx f(l)R\left(\frac{R}{M}\right)^{l+1} \sim 0.07\left(\frac{1.4M_\odot}{M}\right)^3\left(\frac{R}{10km}\right)^4 \sec$$

- For ℓ=2 is ~1.2-4kHz

- Rotation breaks the symmetry: the various **-ℓ≤m≤ℓ** decouple
- There is coupling between the polar and axial modes
- The frequency shifts:

$$\omega_{\text{inert}}(\Omega) = \omega(\Omega = 0) + \kappa m\Omega$$

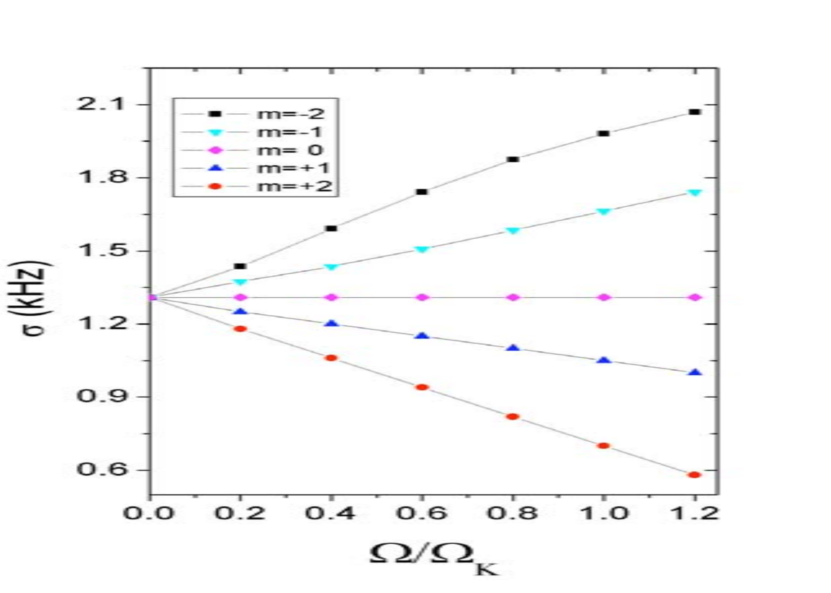

Stavridis & KK 2005

f-mode-(II)

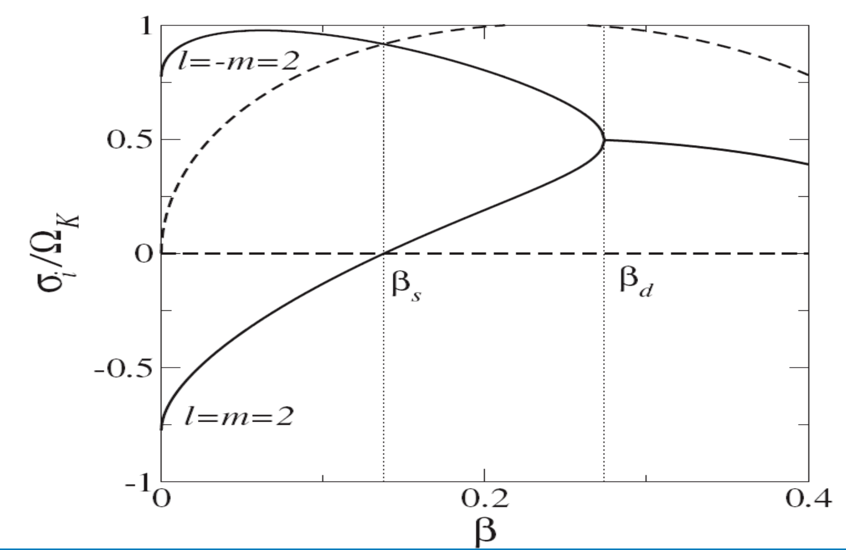

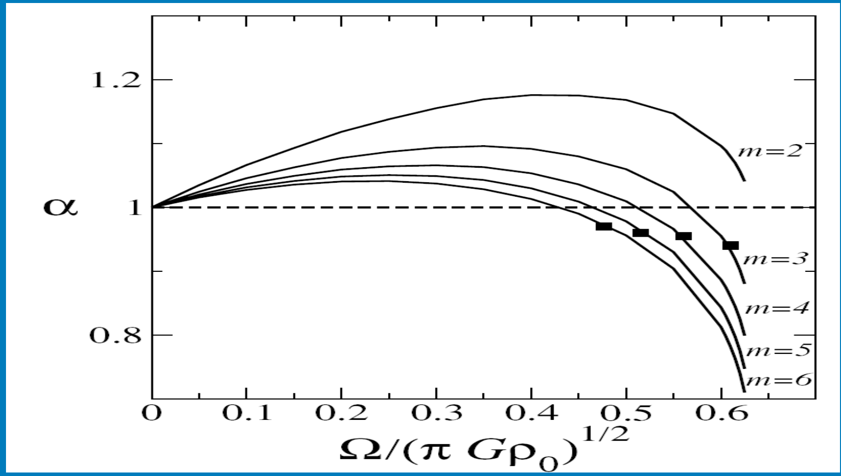

- In Newtonian theory the ***m=2*** f-mode cannot become unstable for ***$\beta<\beta_K$***
- In GR the ***m=2*** f-mode becomes unstable for ***$\Omega>0.85\Omega_K$***

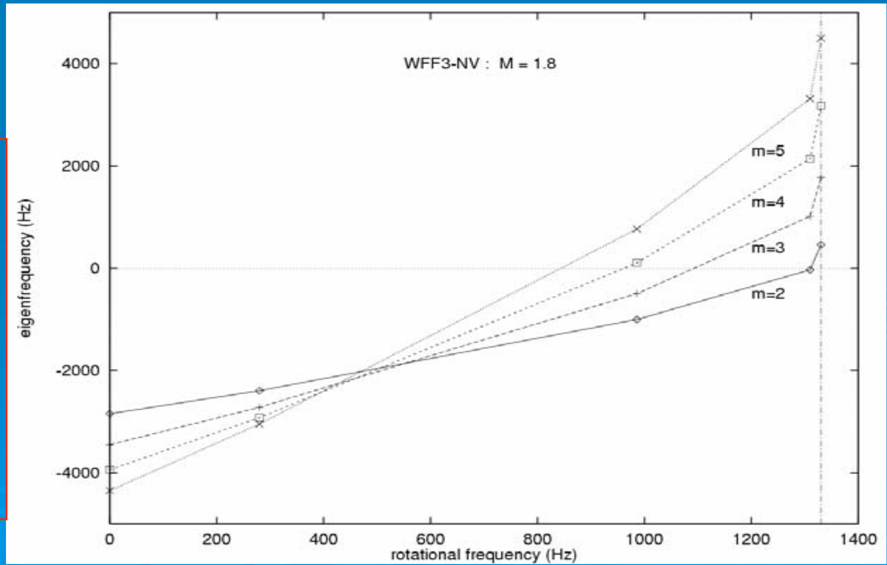

f-mode (astrophysics)

- In GR the ***m=2*** mode becomes unstable for $\Omega > 0.85\Omega_{Kepler}$ or $\beta > 0.06\text{-}0.08$
- Detectable from as far as 15Mpc (LIGO-I), 100Mpc (LIGO-II) (*depending on the saturation amplitude*).
- Differential rotation affects the onset of the instability
- Non-linear calculations by Shibata & Karino (2004) suggest that:
  - Up to 10% of energy and angular momentum will be dissipated by GWs.
  - Amplitude (at ~500Hz):

$$h_{\text{eff}} \sim 5 \times 10^{-22} \left(\frac{R_e}{20km} \right)^{1/4} \left(\frac{M}{1.4 M_\odot} \right)^{3/4} \left(\frac{100\text{Mpc}}{r} \right)$$

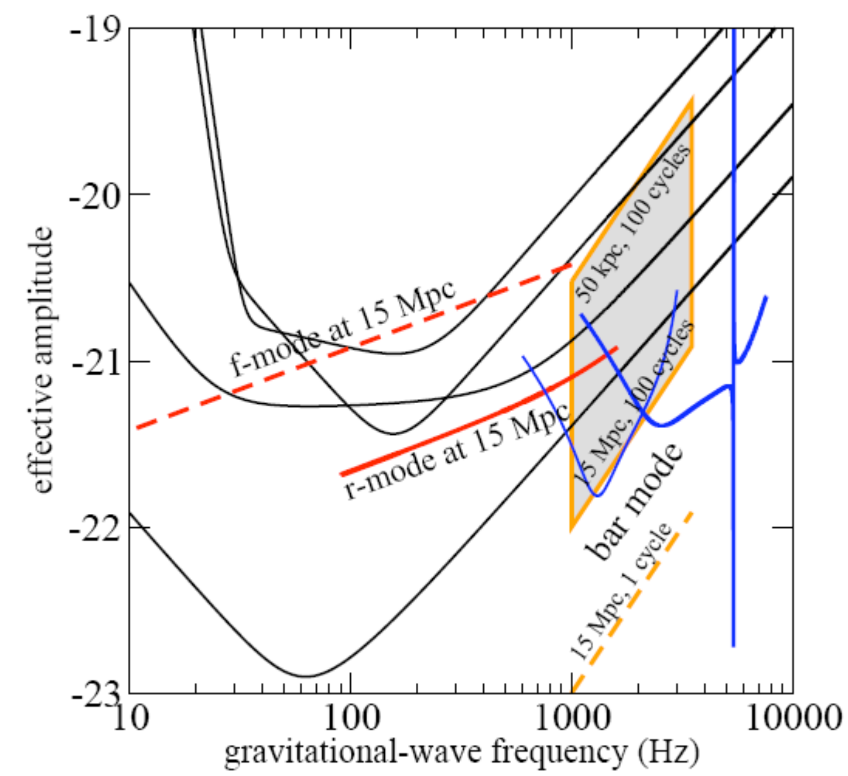

f-mode Instability

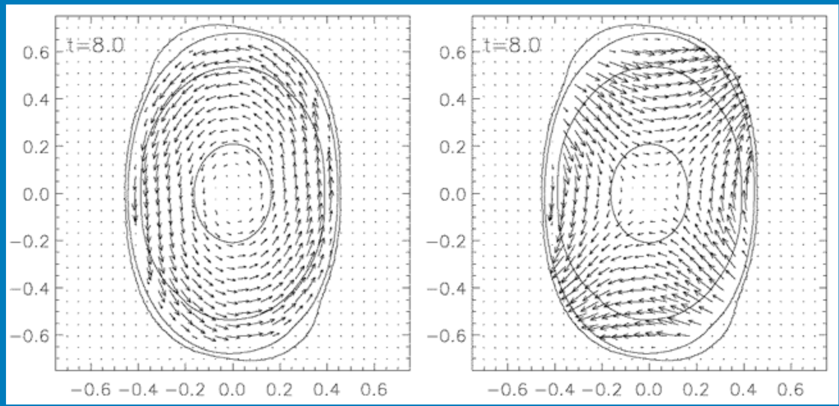

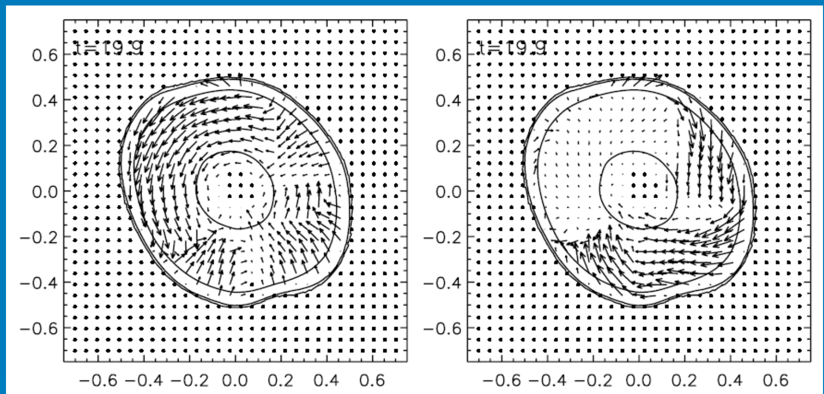

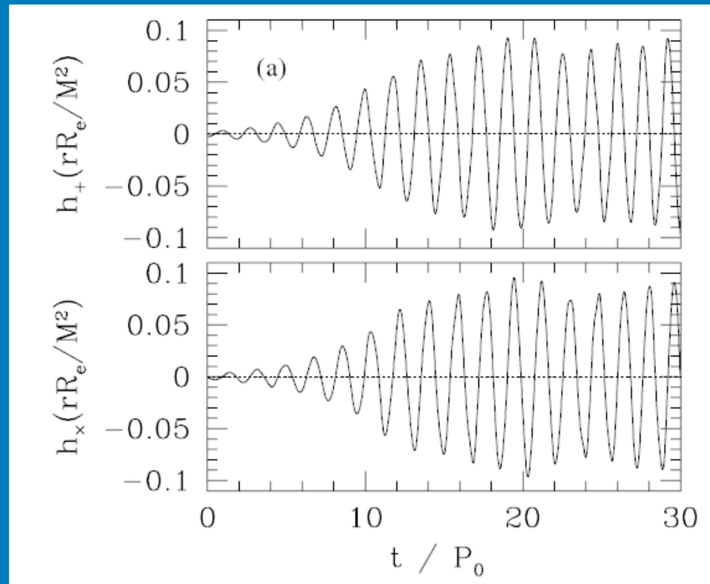

Lai & Shapiro, 1995

Ou, Lindblom & Tohline, 2004

Shibata & Karino, 2004

In the *best-case scenario*, the GWs are easily detectable out to 140 Mpc !

Major uncertainties:

1. Relativistic growth times
2. Nonlinear saturation
3. Initial rotation rates of protoneutron stars – event rate
4. Effect of magnetic fields

Viscosity driven Instability

- For Newtonian polytropic stars the instability can exist only for N<0.808.
- For relativistic polytropic stars N<0.55 (worst)
- It might be possible for fast rotating strange stars!
- The emission of GWs might not allow the instability to grow at all. Compare:

$$\tau_{SV} \sim 10^8 \left(\frac{T}{10^9 K} \right)^2 \mathrm{s} \quad \mathrm{vs} \quad \tau_{GW}^{f-\mathrm{mode}} \sim 0.07s$$

r-modes

- A non-rotating star has only trivial axial modes. Rotation provides a restoring force (Coriolis) and leads in the appearance of the inertial modes. The *l=m=2* inertial mode is called r-mode.
- In a frame rotating with the star, the r-modes have frequency

$$\omega_{\mathrm{rot}} = \frac{2m}{l(l+1)}\Omega$$

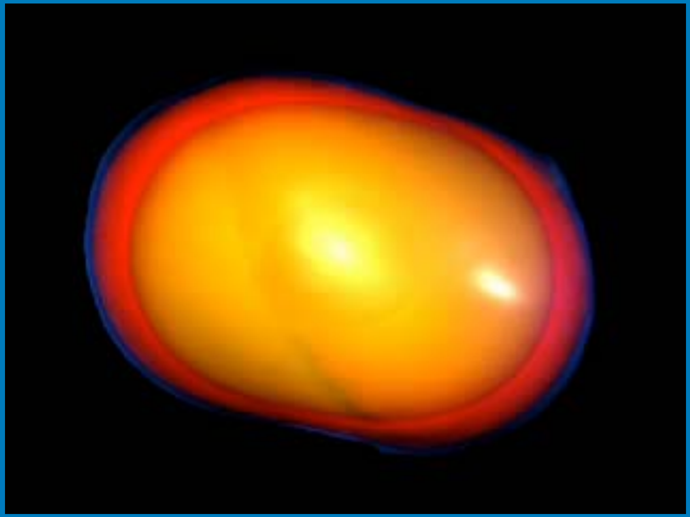

Lindblom-Vallisneri-Tohline

- GW amplitude depends on a (the saturation amplitude).
- Mode coupling might not allow the growth of instability to high amplitudes (Schenk etal)
- The existense of *crust*, hyperons in the core, magnetic fields, affects the efficiency of the instability.
- For newly born neutron stars might be quite weak ; unless we have the creation of a strange star
- Old accreting neutron (or strange) stars, probably the best source! (400-600Hz)

$$h(t) \approx 10^{-20}\alpha\left(\frac{\Omega}{1\ \mathrm{kHz}}\right)\left(\frac{10\mathrm{Kpc}}{d}\right)$$

$$\alpha \simeq 10^{-3} - 10^{-4}$$

R-mode: Instability window

- For the r-mode (ℓ=2) we get:

$$\tau_{BV} \approx 2.4\times10^{10}\left(\frac{1.4M_\odot}{M}\right)\left(\frac{R}{10\mathrm{km}}\right)^5\left(\frac{10^9K}{T}\right)^6\left(\frac{P}{1\mathrm{ms}}\right)^2 \mathrm{sec}$$

$$\tau_{SV} \approx 1.2\times10^{8}\left(\frac{1.4M_\odot}{M}\right)^{5/4}\left(\frac{R}{10\mathrm{km}}\right)^{23/4}\left(\frac{T}{10^9K}\right)^2 \mathrm{sec}$$

$$\tau_{GW} \approx -22\left(\frac{1.4M_\odot}{M}\right)\left(\frac{R}{10\mathrm{km}}\right)^{-4}\left(\frac{P}{1\mathrm{ms}}\right)^6 \mathrm{sec}$$

The instability will grow if

$$\tau_{visc}(\Omega,T) \geq \tau_{inst}(\Omega)$$

The $l=m=2$ r-mode grows on a timescale 20-50secs

- Instability window
- Many astrophysical applications both on newly born and old NS

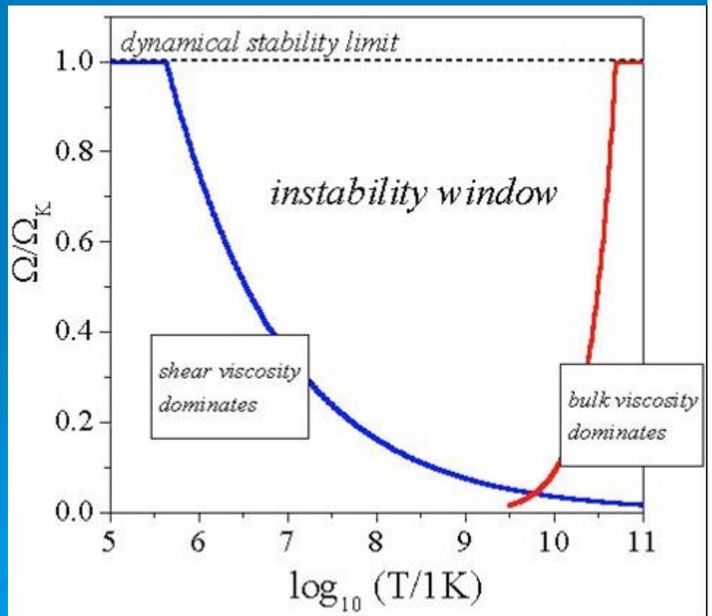

R-mode instability vs EOS

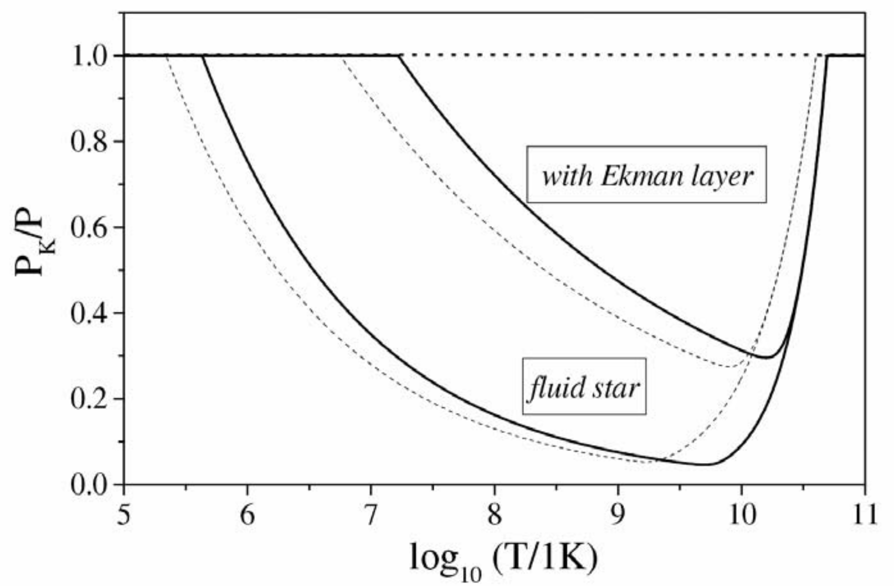

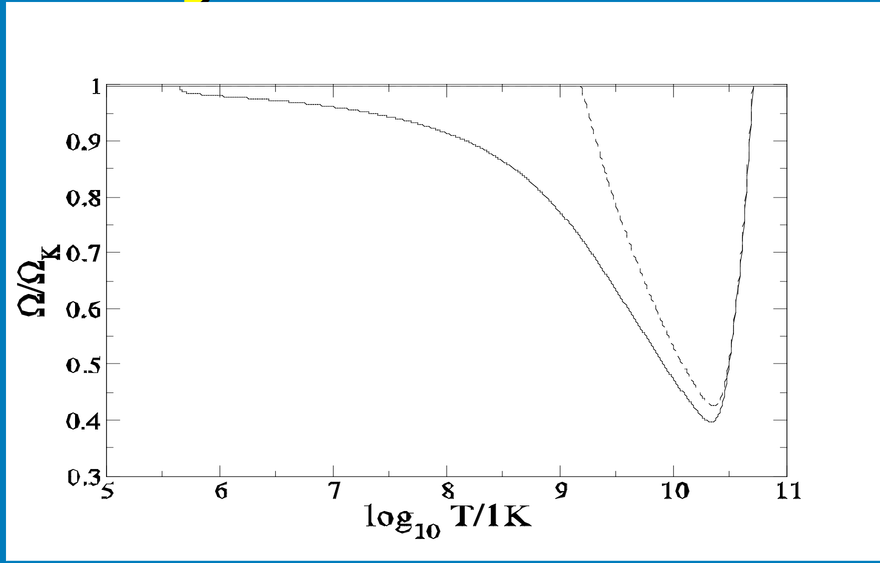

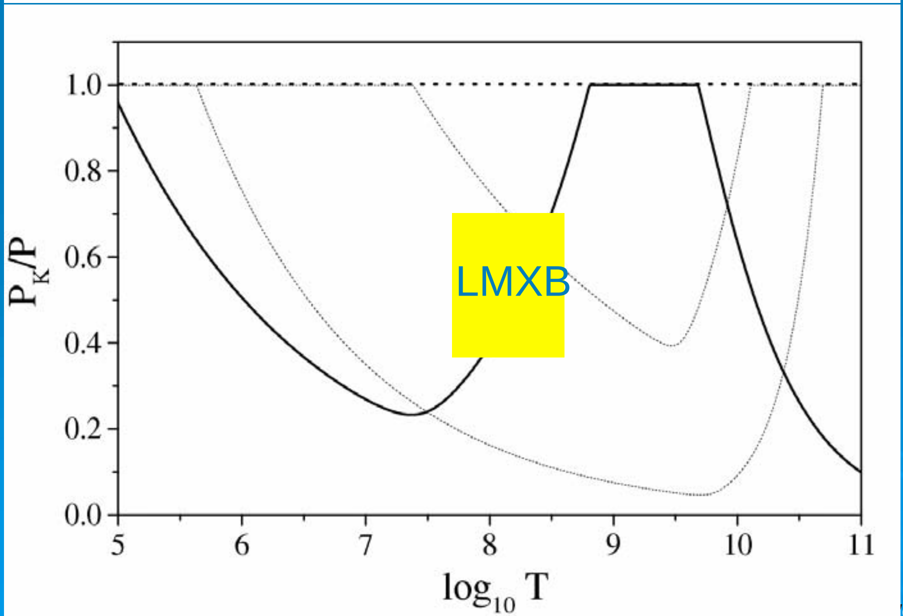

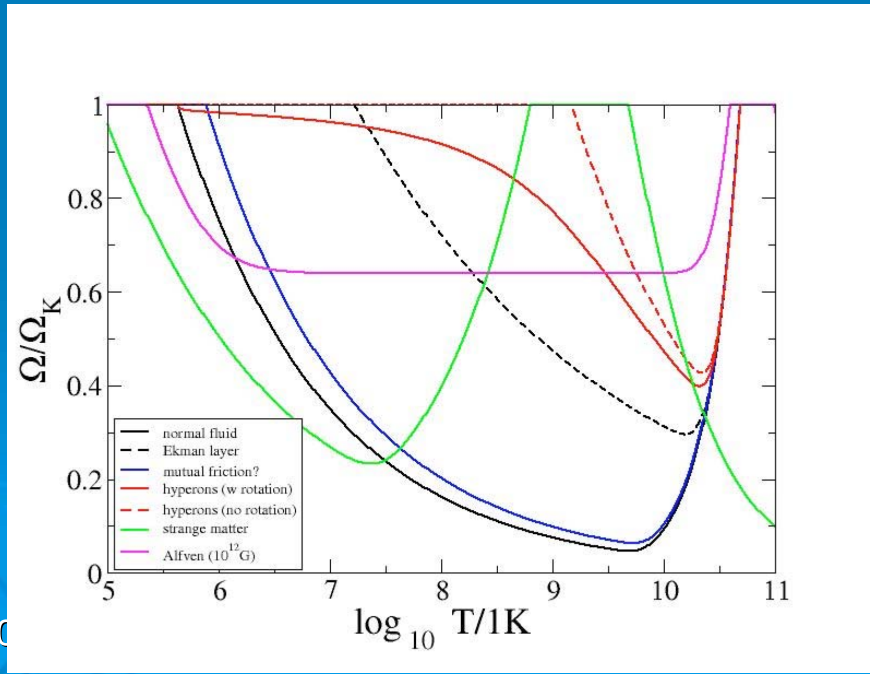

Saturation of Nonlinear R-Modes

Long-term nonlinear evolution of r-mode grown to O(1), using accelerated gravitational-radiation-reaction force.

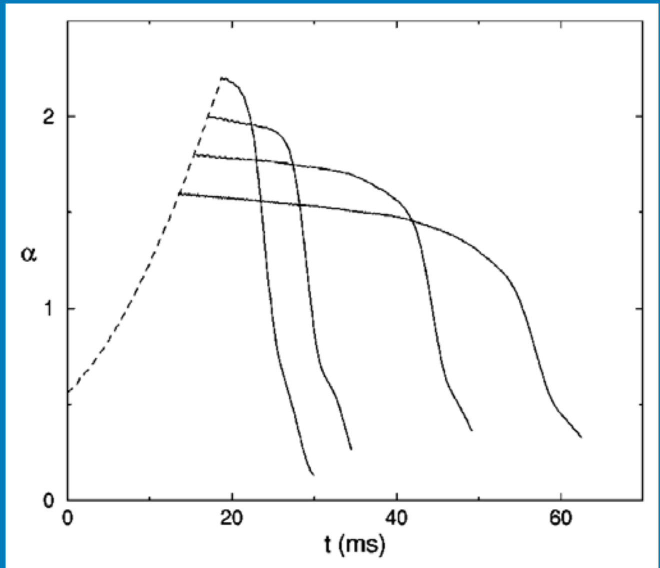

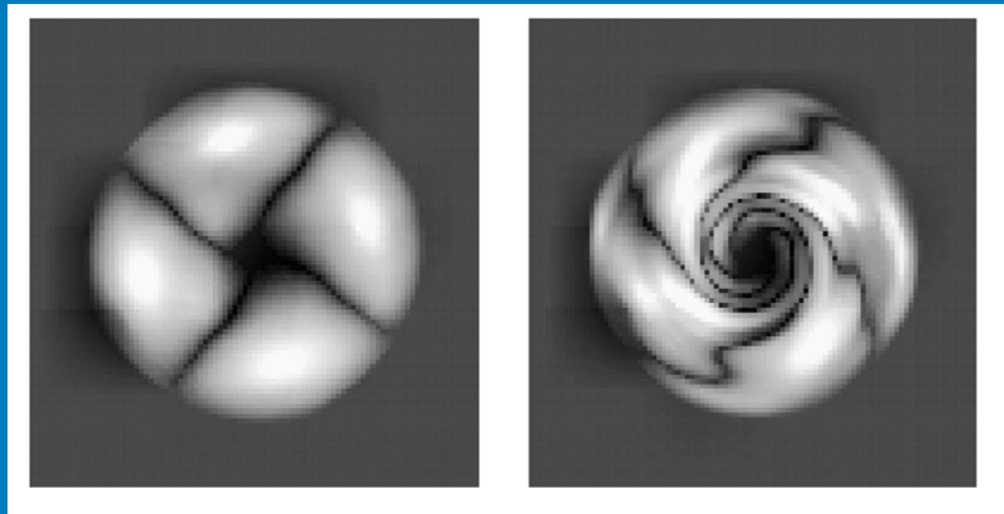

Gressman, Lin, Suen, Stergioulas & Friedman (2002)

- When r-mode exceeds its saturation amplitude, it ultimately breaks down into a vortex-like motion.
- More detailed analysis by Lin & Suen (2004) showed that this break-down is due to nonlinear 3-mode coupling of the r-mode to two other inertial modes. Saturation amplitude of $O(10^{-2})$.
- However, resolution not sufficient to resolve inertial modes with very high mode number.

Saturation of Nonlinear R-Modes

Morsink (2002)
Schenk, Arras, Flanagan, Teukolsky, Wasserman (2002)
Arras, Flanagan, Morsink, Schenk, Teukolsky, Wasserman (2003
Brink, Teukolsky, Wasserman (2004a, 2004b,2007)

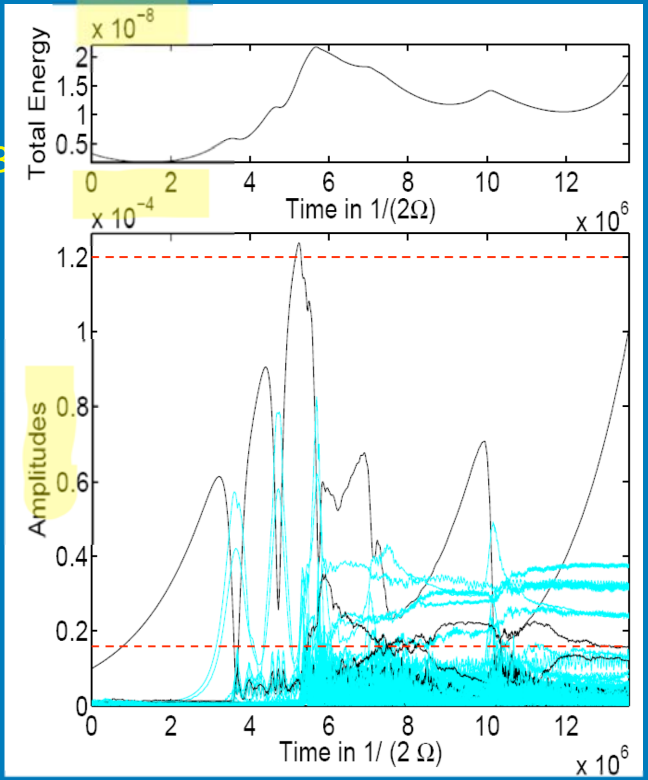

Second-order perturbative evolutions (Newtonian).

Several *3-mode couplings* of r-mode to other *high-order inertial modes*.

Saturation amplitude may be of O(10^{-3}-10^{-4}), *still fine* for *GWs from LMXBs*.

(see Andersson, Jones, KK & Stergioulas, 2001)

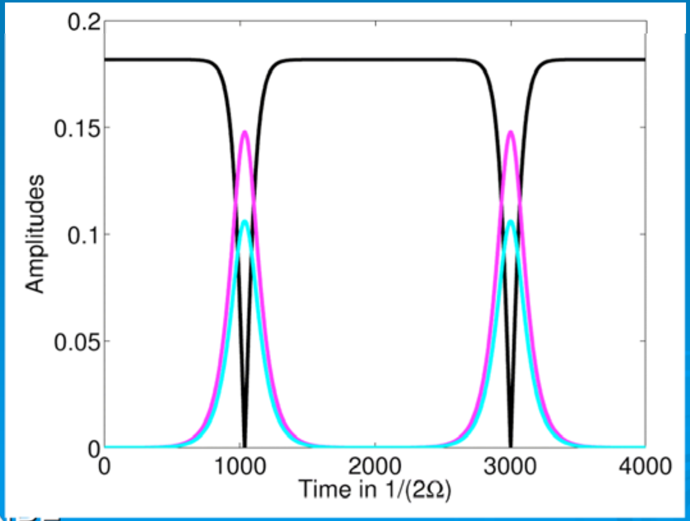

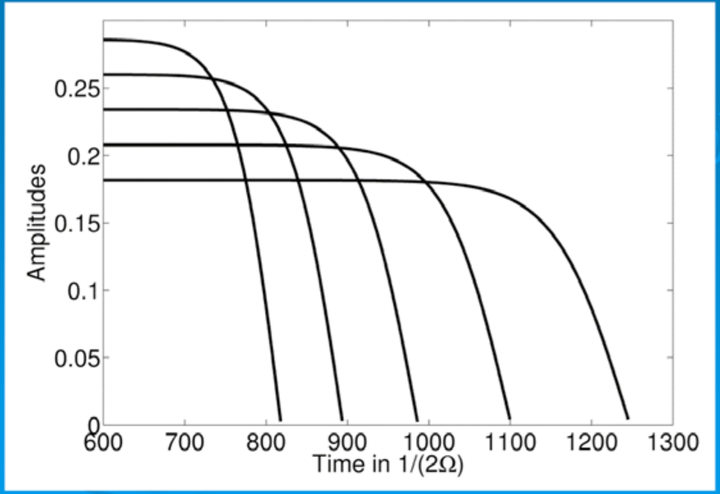

LMXBs & r-modes

Limiting Period : 1.5ms
Fastest known pulsar: 1.56ms

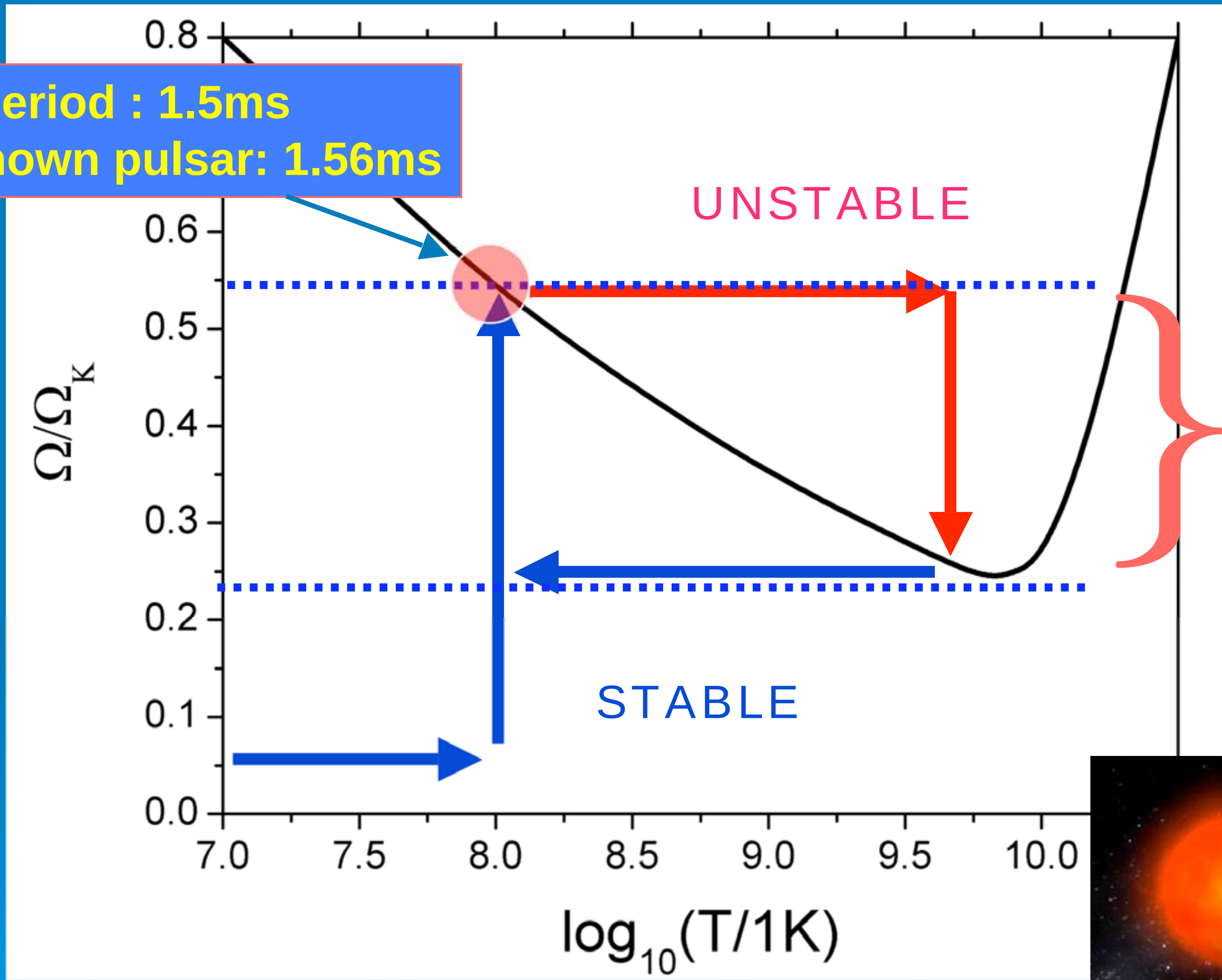

Period clustering of ms pulsars

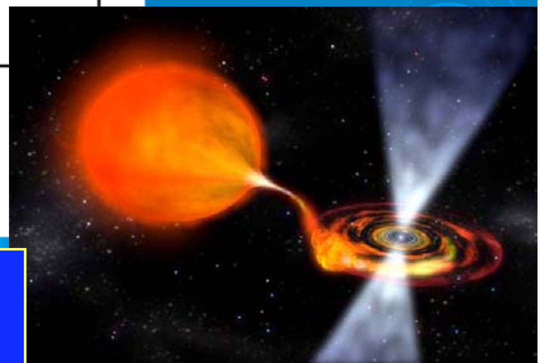

Andersson, KK, Stergioulas 1999, Levin 2000
Andersson, Jones, KK, Stergioulas 2000, Heyl 2002

r-modes in young strange stars

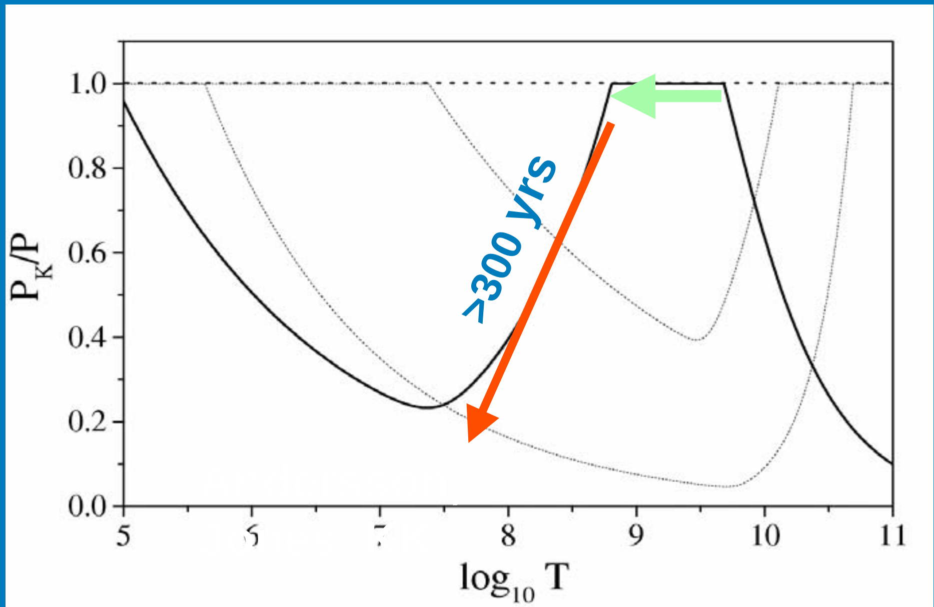

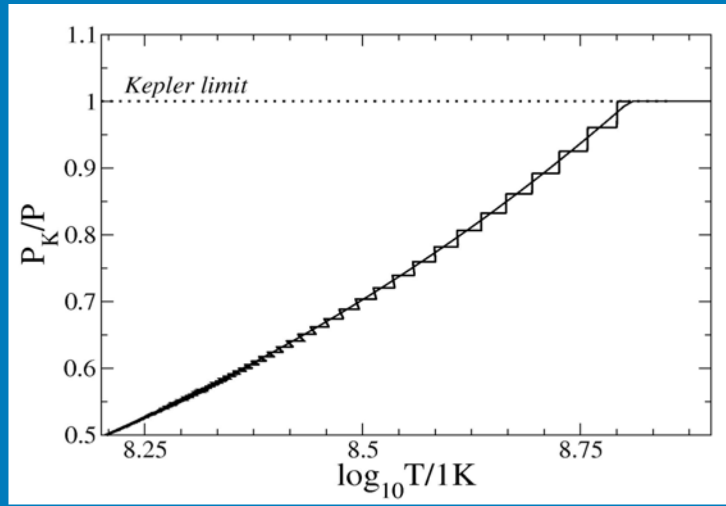

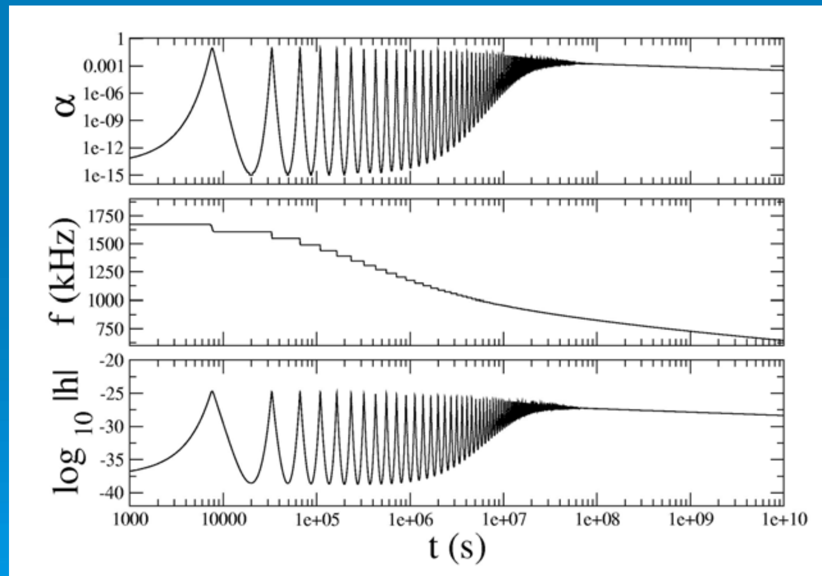

- Lasts for more than ~ 300yrs
- A few weeks: h_{eff}~10^{-21} (r~10kpc)
- 5-10 might be active in our Galaxy!

Unique signature

Andresson,Jones, KK (2002)

w-modes

Very high frequency (short lived) modes 6-12kHz
(KK & Schutz 1986,1992, Leins etal 1993)

The frequency of the w-modes show a very accurate *scaling behavior* for a large sample of realistic EOSs. **(KK, Apostolatos & Andersson 2001)**

W-modes of rotating stars in slow rotation and in Inverse Cowling Approximation (ICA) have been calculated
(Stavridis & KK 2005, Stegioulas, Hawke, KK 2006)

W-modes of ultra compact stars R<3M become CFS unstable for small rotational rates ***Ω > 0.20 Ω_{Kepler}*** (ergoregion instability)
(KK, Ruoff & Andersson 2004)

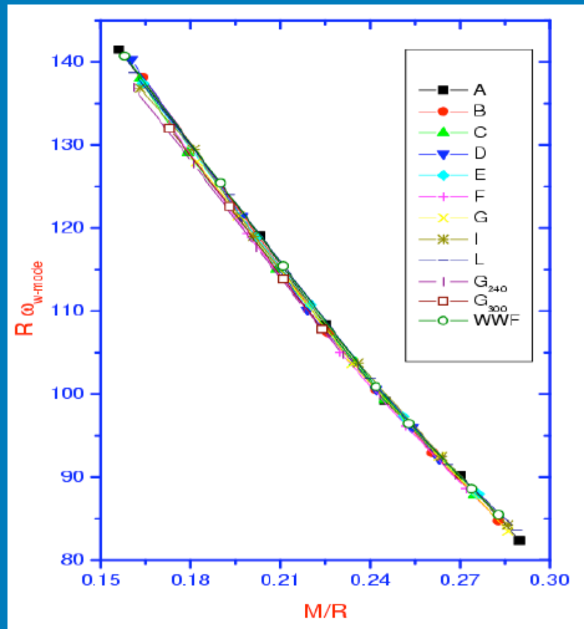

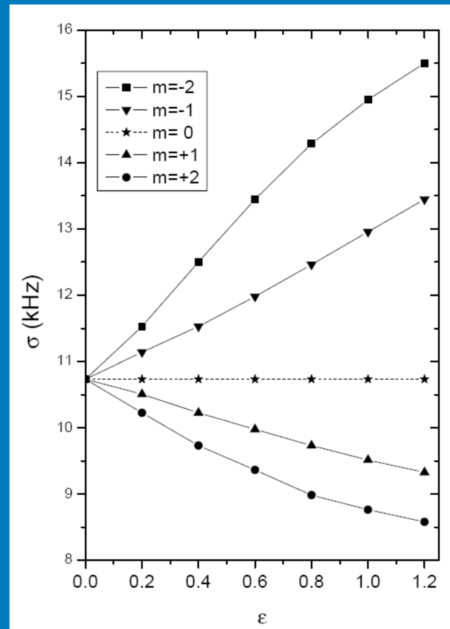

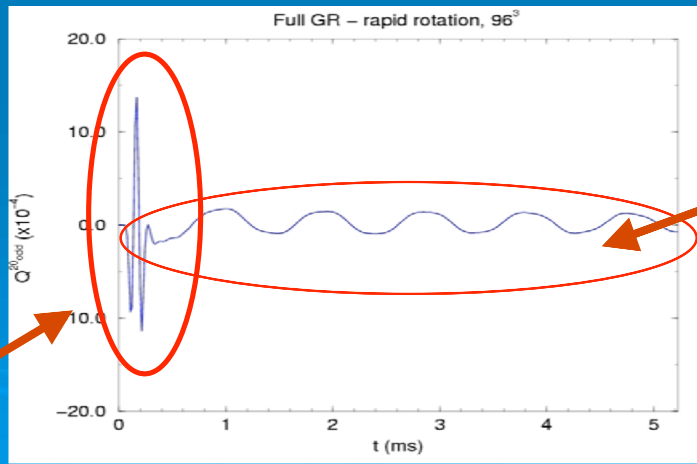

F-mode

W-mode

Bar-mode dynamical instability (I)

•For rapidly (differentially!) rotating stars with:

$$\beta = \frac{T}{|W|} \sim \frac{1}{R} > \beta_{\rm dyn} \approx 0.27$$

•The "bar-mode" grows on a dynamical timescale.

$$h \approx 9\times10^{-23}\left(\frac{\varepsilon}{0.2}\right)\left(\frac{f}{3\ \rm kHz}\right)^2\left(\frac{15\ \rm Mpc}{\rm d}\right)M_{1.4}R_{10}^2$$

•If the bar persists for many (~10-100) rotation periods, the signal will be easily detectable from at least Virgo cluster.

–A considerable number of events per year in Virgo: ≤10^{-2} /yr/Galaxy

–**Typical Frequencies ~1.5-3.5kHz**

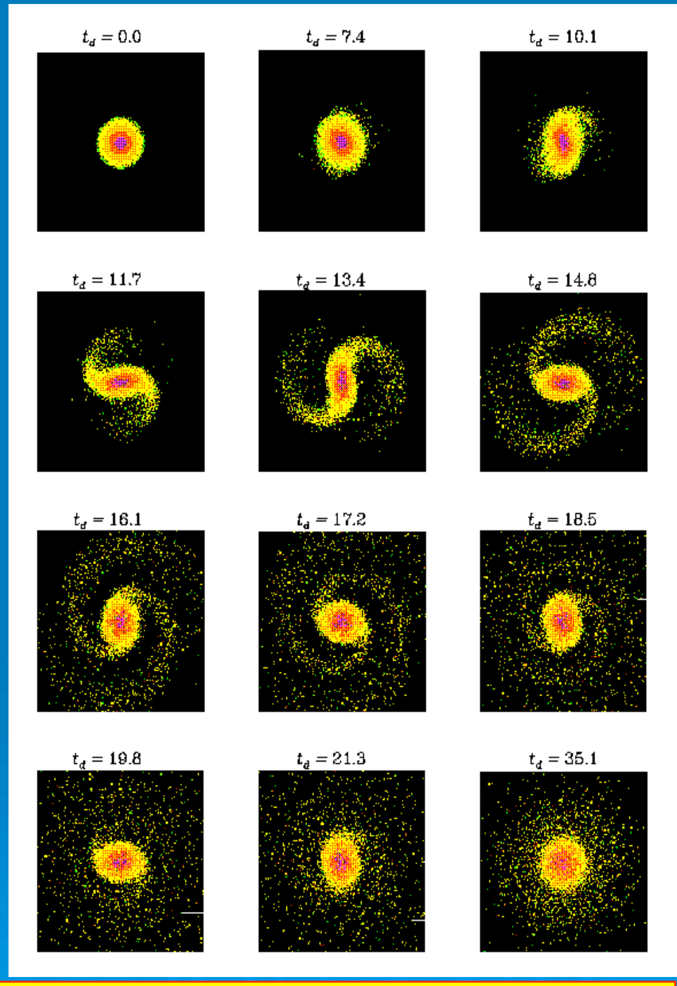

Remember Spherical Detectors: f_0~3.2kHz

Bar Mode Dynamical Instability (III)

- Bars can be also created during the merging of NS-NS, BH-NS, BH-WD and Collapsars (type II).
- GR enhances the onset of the instability ($\beta_{dyn} \gtrsim 0.24$) and β decreases with increasing M/R.
- Bar-mode instability might happen for much smaller β if centrifugal forces produce a peak in the density off the source's rotational center.
- Highly differentially rotating stars are shown to be dynamically unstable for significantly lower β (even when $\beta \gtrsim 0.01$).

$$h_{eff} \simeq 3\times10^{-22}\left(\frac{f}{800Hz}\right)^{1/2}\left(\frac{R_{eq}}{30km}\right)\left(\frac{M}{1.4M_{\odot}}\right)^{1/2}\left(\frac{100Mpc}{d}\right)$$

- Bars can be also create during the collapse of a SMS before the creation of a SMBH. Ideal sources for LISA.

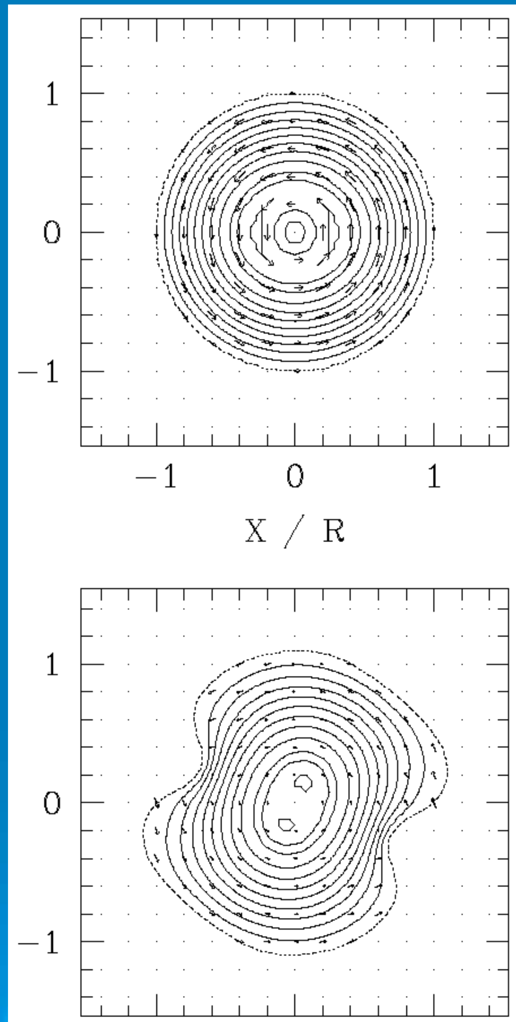

Shibata-Karino-Eriguchi

Dynamical instability (m=1)

- Numerical simulations have shown the existence of an one arm (m=1) dynamical instability for *$\beta << 0.14$* !!! (Centrella etal 2001)
- The nature of this instability is not yet well understood!
- An unstable m=1 mode triggers a secondary m=2 bar mode of smaller amplitude and the bar mode excite it persists for only a few rotations
- The emitted GWs have smaller amplitudes than those emitted by stars unstable to the m=2 bar mode (Saijo et.al. 2003)

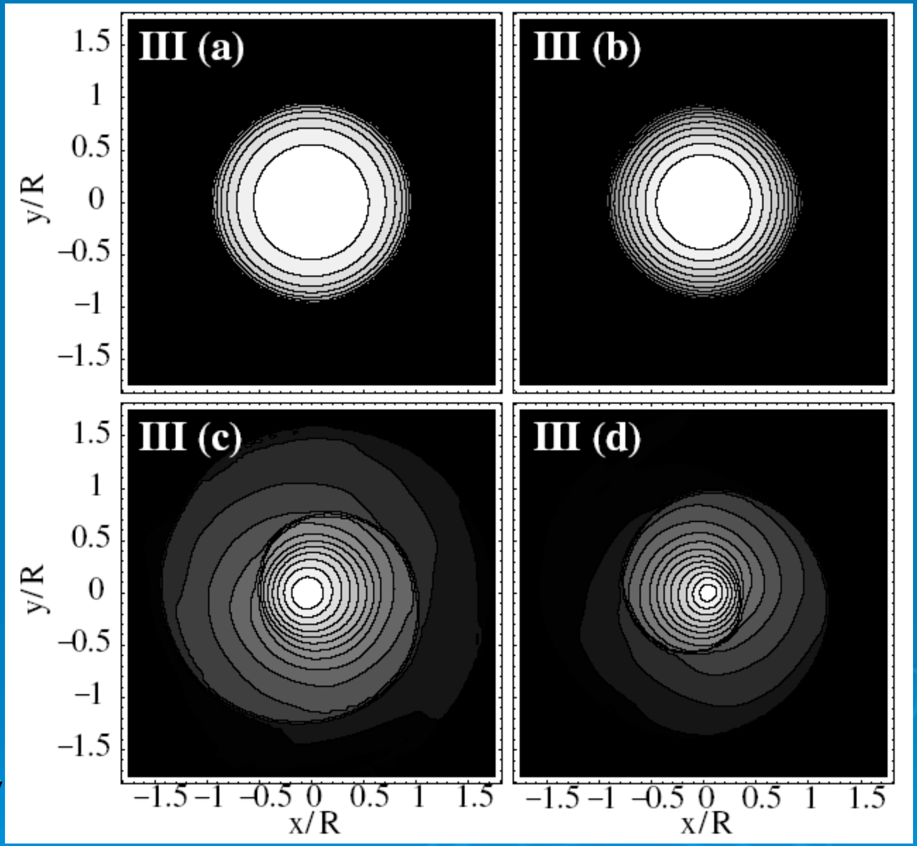

Soft Gamma Repeaters (SGR) & Stellar Oscillations

- The Soft gamma Repeaters (SGRs) are objects exhibiting recurrent bouts of γ-ray flare activity. They thought to be **magnetars** i.e. neutron stars with strong magnetic field $>10^{14}$ G.
- **SGRs exhibit giant flares (10^{44}-10^{46} ergs/s)**
- The catastrophic magnetic instability that powers the giant flares is thought to be associated with large-scale fracturing of NS crust.
- **Global seismic (23 mag) vibrations are excited.**
- **Pulsations are visible in the tail and reveal the neutron star period.**
- **3** such flares have been detected from satellite high-energy detectors.

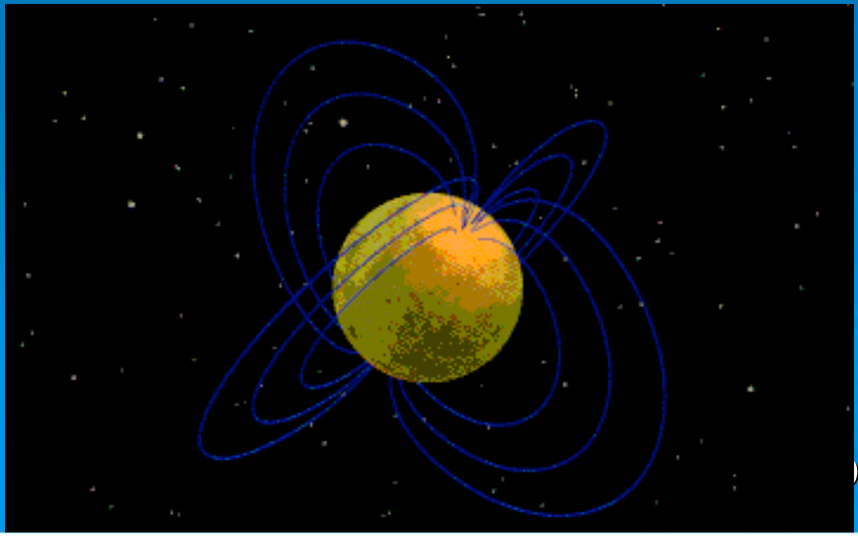

6 more potential candidates are known (anomalous X-ray pulsars)

The Dec 2004 flare from SGR 1806-20 was the most energetic ever recorded (Rossi X-ray Timing Explorer, RXTE).

The P-P_{dot} diagram

$$B = 3.2 \times 10^{19} \sqrt{\dot{P}P} G$$

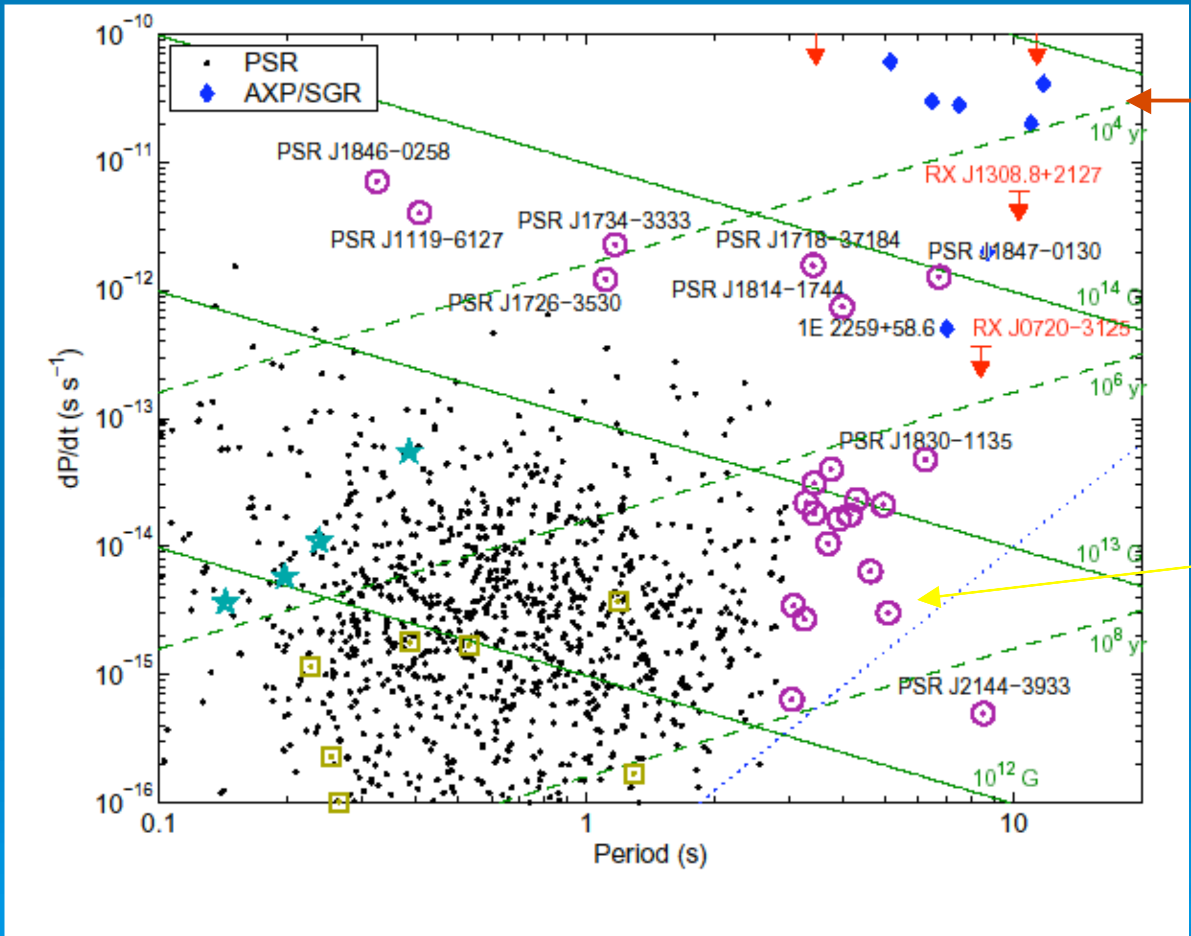

SGRs, AXPs

main
radio pulsar
population

Approximate Distances
and
Typical Luminosities

SGR1900+14	10 kpc
SGR1627-41	11 kpc
SGR1806-20	14 kpc
SGR0525-66	50 kpc

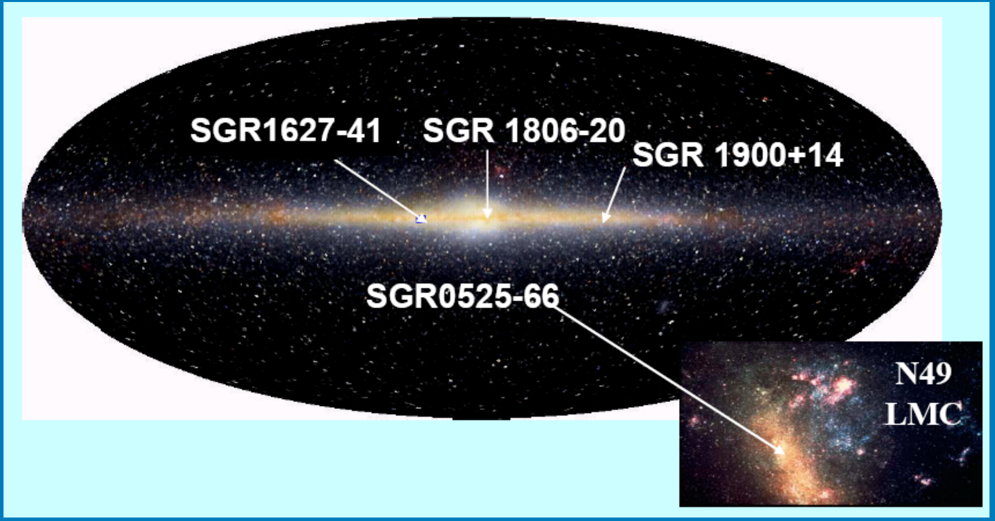

Short burst	0.1 s	10^{40} erg/s
Intermediate burst	7 s	5×10^{41} erg/s
Giant flare	300 s	10^{43} -10^{47} erg/s
Persistent X-rays	---	10^{36} erg/s

Relevant modes

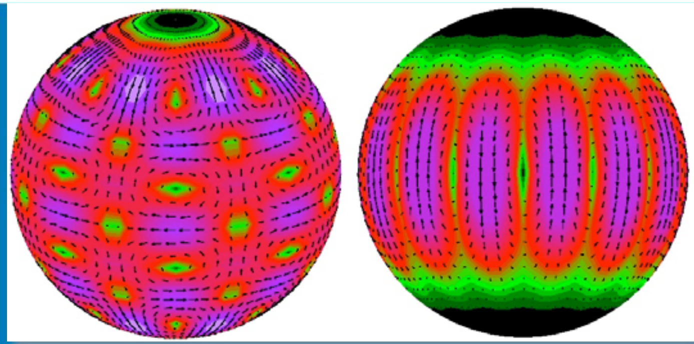

- t-modes (torsional)
  - normal modes of elastic waves in the solid crust
  - Typical frequency **$\sigma \sim u_s/R$**
- r-modes (?)
  - induced by rotation, Coriolis is the restoring force
  - Typical frequency **$\sigma \sim \Omega$**
- s-modes : result from crustal elasticity, they are shear waves in the solid NS crust
  - Typical frequencies from few 100 Hz
- i-modes : interface modes (typical frequencies ~ 10-30 Hz)
- Alfven modes : oscillations of the B-field
- Magnetic field and rotation shift and split the spectra

$$\sigma \approx \sigma_0 + \alpha \cdot B + \beta \cdot \Omega$$

- All these types of modes become CFS unstable

Observations

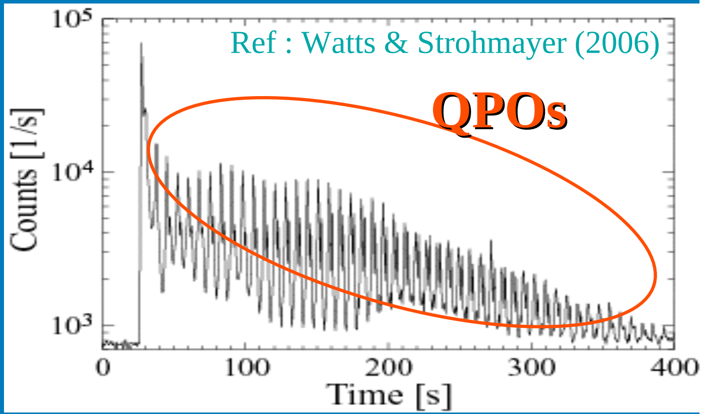

- **Giant flares in SGRs**
  - Up to now, three giant flares have been detected.
    - *SGR 0526-66 in 1979, SGR 1900+14 in 1998, SGR 1806-20 in 2004*
  - Peak luminosities : 10^{44} – 10^{46} erg/s
  - A decaying tail for several hundred seconds follows the flare.
- **QPOs in decaying tail** (Israel *et al*. 2005; Watts & Strohmayer 2005, 2006)
  - SGR 1900+14 : 28, 54, 84, and 155 Hz
  - SGR 1806-20 : 18, 26, 29, 92.5, 150, 626.5, and 1837 Hz (possible additional frequencies : 720 and 2384 Hz)

Pure Crust Torsional Modes

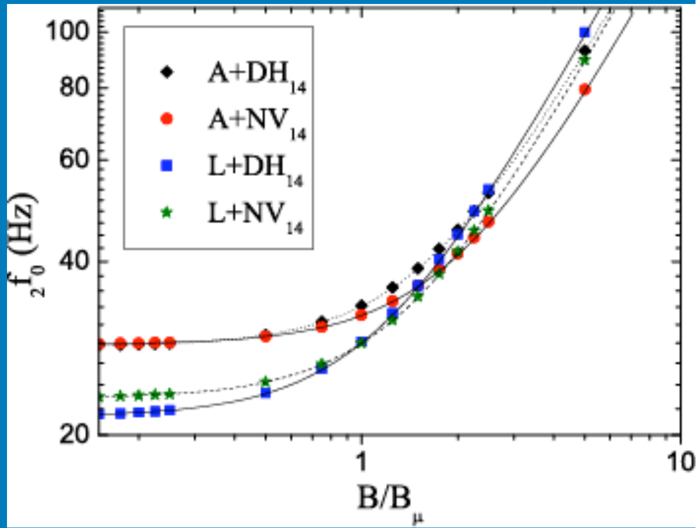

NON-MAGNETIZED CASE

$$_\ell f_0 \approx \sqrt{\ell(\ell+1)}\,\frac{u_s}{R}$$

- For fundamental modes
  - *Frequencies depend on the stellar parameters.*
    → they can vary by up to 30 ~ 50 %
  - *The GR periods 15-30% off the Newtonian ones*
  - *The crust EOS does not affect significantly (1~5%)*
- For overtones
  - *Frequencies are practically independent of the harmonic index* ℓ
  - *The variations in the frequencies due to different choices of both the high-density and crust EOS are significant.*
    → ex) frequencies of first overtones vary the range of 500 – 1200 Hz.

THE EFFECT OF THE MAGNETIC FIELDS

- We derive the empirical formula such as
  where $B_\mu = 4 \times 10^{15}$ G
- For $B > B_\mu$, the shift in the frequencies is significant.

$$\frac{_\ell f_n}{_\ell f_n^{(0)}} \sim \left[1 + {_\ell\alpha_n}\left(\frac{B}{B_\mu}\right)^2\right]^{1/2}$$

…higher harmonics?

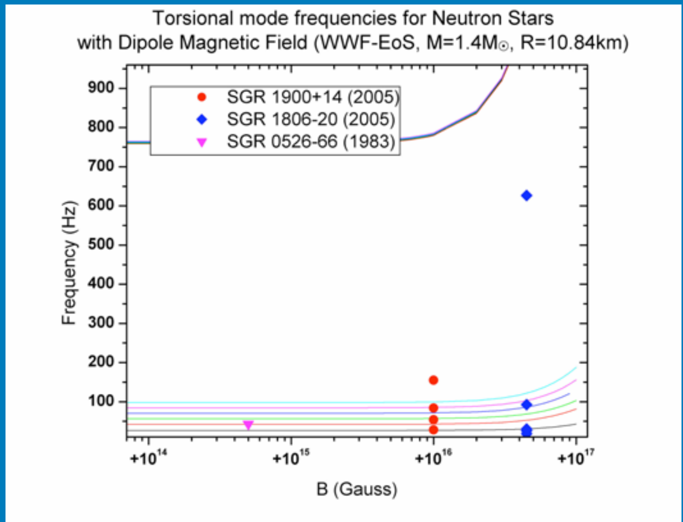

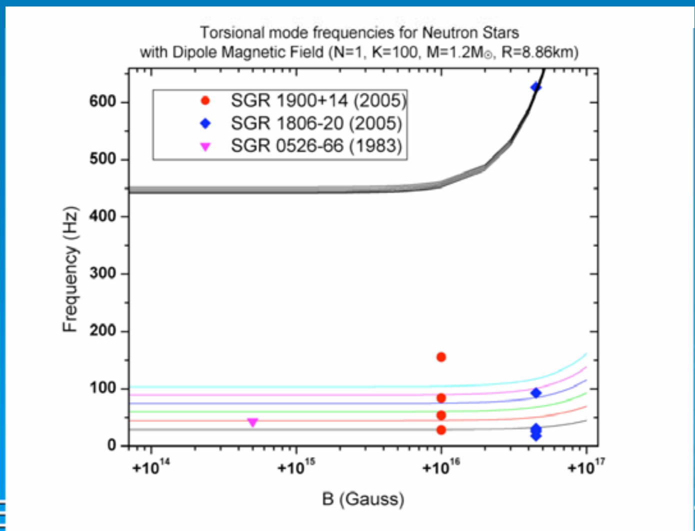

- **Higher overtones are also present e.g. 626.5 and 1840 Hz!**
- **They are independent from angular index ℓ**
- **<u>Unique</u> information about the thickness of the crust.**

$$\frac{\Delta r}{R} \approx \frac{n\pi}{\sqrt{\ell(\ell+1)}} \frac{{}_{\ell}f_0}{{}_{\ell}f_n} \left(\frac{R}{u_s} \right)$$

Attempt to fit to Observational data

- Some of the stiff models fit quite well to the observational data
  - SGR 1900+14 : L+NV$_{25}$ (28, 54, 84, 155 Hz → ${}_3t_0$, ${}_6t_0$, ${}_9t_0$, ${}_{17}t_0$)
  - SGR 1806-20 : L+DH$_{17}$ or L+NV$_{20}$
    (18, 29, 92.5, 150, 626.5, 1837 Hz → ${}_2t_0$, ${}_3t_0$, ${}_9t_0$, ${}_{15}t_0$, ${}_lt_1$, ${}_lt_4$)

  c.f.) without magnetic fields and Newtonian case :

$$ {}_\ell t_0 \sim \frac{\sqrt{\ell(\ell+1)}u_s}{2\pi R} $$

- However …
  - it is difficult to explain the observational data of 26 Hz, because this mode is very close to another at 29 Hz.
  - It is difficult to fit in the data the 18Hz mode
  - Similarly, the spacing between the 626.5 and 720 Hz in SGR 1806-20 may be too small to be explained by consecutive overtones of crust modes.

  → it may be difficult to explain all frequencies by pure crust torsional modes!!

  → **It is necessary to consider the global Alfven modes !!**

Comparison with Observational data

$$ {}_{\ell}a_0 \approx {}_2\beta_0 \sqrt{\frac{\ell}{2}} \left(\frac{B}{B_\mu} \right) $$

- All observational data can be explained by global Alfven modes !

  → Owing to the non-degenerate of overtones for different values of ℓ

  ex) SGR 1806-20 : *B/Bμ~1.25*

  SGR 1900+14 :*B/Bμ~1.94*

  for A+DH$_{14}$ stellar model.

  → for other stellar models it is easy to fit !!

  - Of course, this magnetic field is strong.

  → it is easier to fit for the weaker magnetic fields, because there exist more modes.

  Ex) SGR 1806-20 : L+NV$_{18}$ with *B/Bμ~0.60*

  → ${}_4a_0$, ${}_8a_0$, ${}_{10}a_0$, ${}_2a_6$, and ${}_2a_{11}$ for *f* < 150 Hz

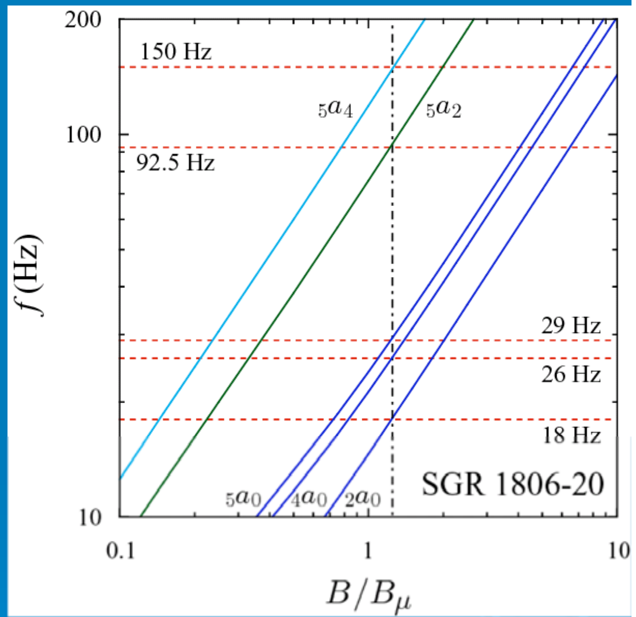

- An upper limit for the strength of magnetic fields can be set !!
  - (0.8 ~ 1.2) x 10^{16} [G]

Torsional modes are CFS unstable

- Perturbation eqn

$$\ddot{Z} = v_s^2 e^{2\nu-2\lambda}\left[Z'' + \left(\frac{4}{r}+\nu'-\lambda'+\frac{\mu'}{\mu}\right)Z' - e^{2\lambda}\frac{\Lambda-2}{r^2}Z\right] + 2im\varpi\left[\frac{1}{\Lambda}+v_s^2\left(1-\frac{2}{\Lambda}\right)\right]\dot{Z},$$

- Approximate formula

$${}_\ell\sigma_n = {}_\ell\sigma_n{}^{(0)}\sqrt{1+\left[\frac{1}{{}_\ell\sigma_n{}^{(0)}}\frac{m\Omega}{\ell(\ell+1)}\right]^2} - \frac{m\Omega(\ell^2+\ell-1)}{\ell(\ell+1)}$$

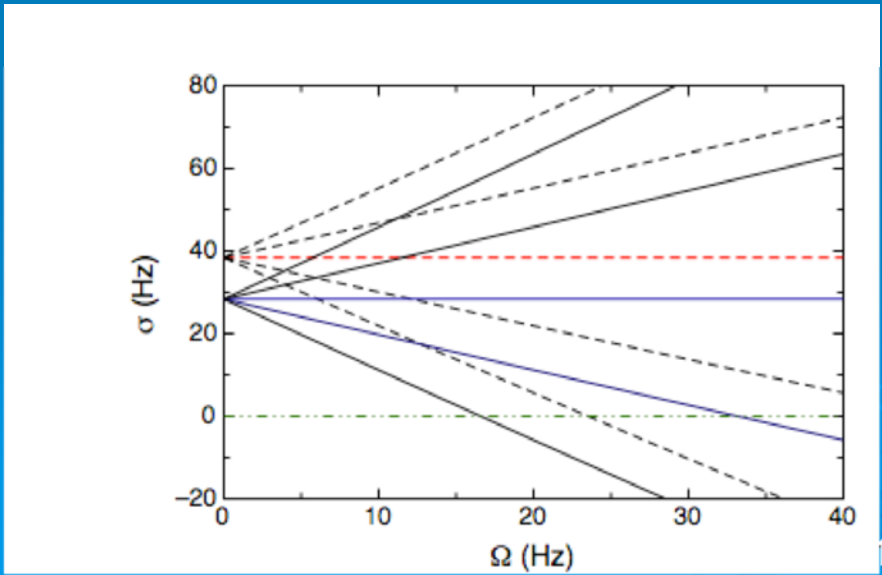

If magnetar born with $\Omega \geq 50$Hz the crust modes will be potentially CFS unstable for hundreds of years working together with the B-field in breaking the crust.

Torsional Modes and GWs

The torsional modes of the NS crust are not likely to be significant source of GWs. For an oscillation with l=2 the gravitational wave strain is estimated to be:

$$h \sim 10^{-25} - 10^{-28} \times \left(\frac{10kpc}{r} \right) \left(\frac{\beta}{10^{-3}} \right)$$

The strong magnetic field might/could couple these surface modes with core oscillations which could emit significantly stronger GWs.

- **The Dec 2004 flare from SGR 1806-20 was the most energetic ever recorded.**
- **LIGO was in operation at that specific period (with a sensitivity far bellow the designed one), the analysis of the data did not show any sign of incoming GWs.**

GW and SGRs

- The energy relesed during the 2004 hyperflare is of the order of 8×10^{46} - 3×10^{47} erg (4×10^{-8} - $2 \times 10^{-7}\ M_{\odot} c^2$)
- If the same amount of energy was released in GWs then the signal would have been marginally detectable by LIGO
- Sensitivity in 2004 about 8 times smaller than H1

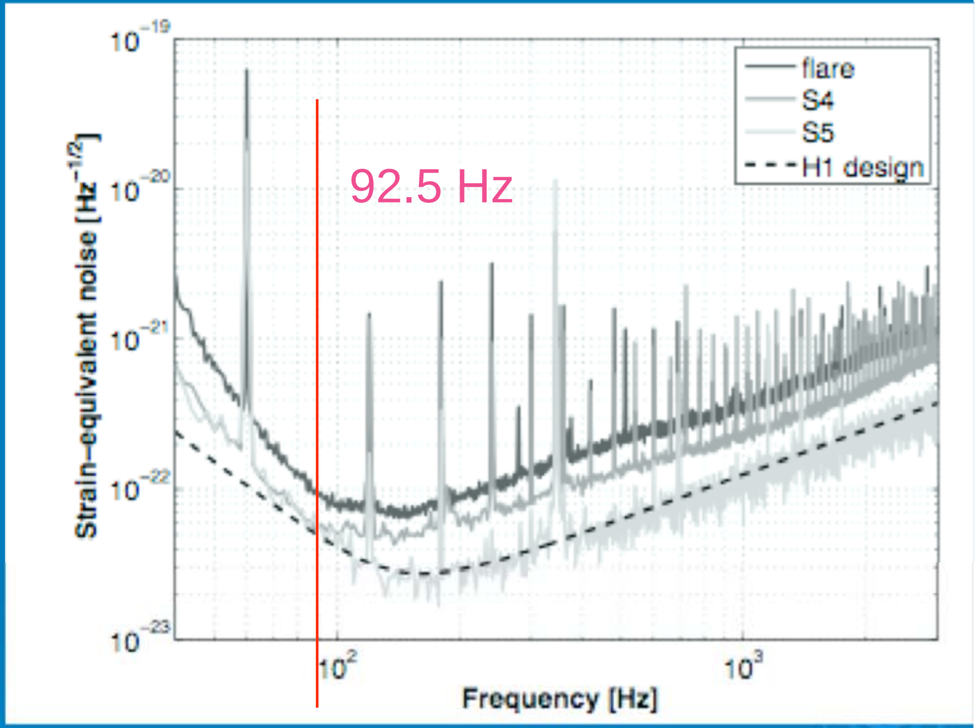

$$E_{GW}^{iso,90\%} = 4.3 \times 10^{-8} M_{sun} c^2 \times \left(\frac{r}{10\text{kpc}} \right)^2 \left(\frac{f_{QPO}}{92.5\text{Hz}} \right)^2 \left(\frac{h_{rss-\det}^{90\%}}{4.5 \times 10^{-22}\ \text{strain Hz}^{-1/2}} \right)$$

AURIGA and the flare

- was optimally oriented towards 1806-20 at the flare time
- was performing as a stationary gaussian detector
- was covering a 100 Hz band in which neutron star f-modes *may* fall(?)

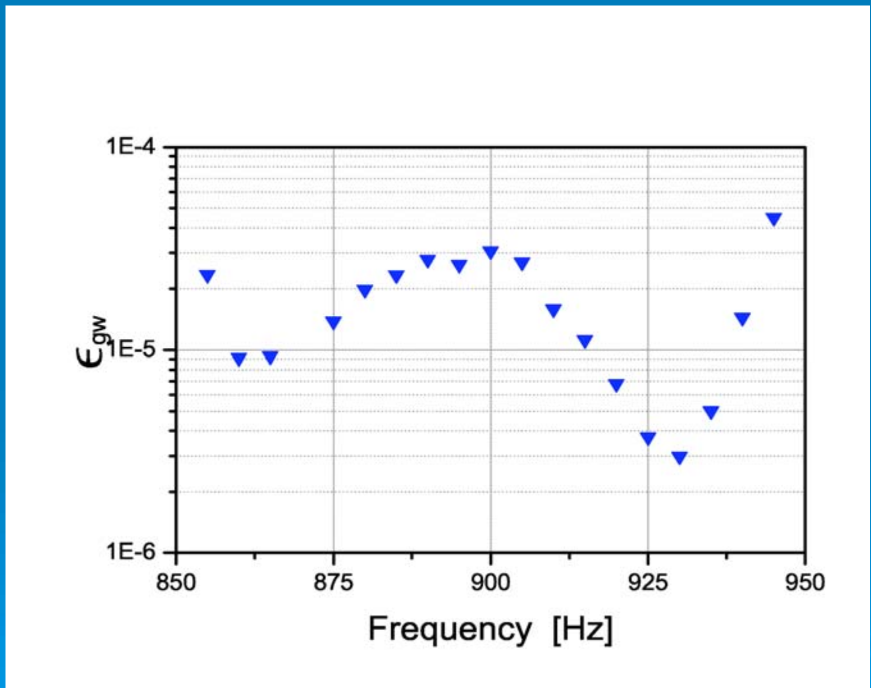

Upper limits on emitted GW energy as fraction of solar mass over the sub-band at frequency f of width Δf models predict :
$E_{gw} \sim 5 \times 10^{-6} M_{\odot}$

At AURIGA's bandwith one can detect:
higher (n,l) t-modes BUT lower s-modes

Open Questions I

1. Detail understanding of the way that the B-field builds up i.e. what type of supernova produces a magnetar?
2. Magnetar population in our Galaxy
3. What is the magnetar birthrate?
4. Relation between giant flares and short GRBs
   - Viewed from a large distance, only the initial spike would be visible
   - It will resemble a short GRB
   - It could be detected out to 100 Mpc

Open Questions II

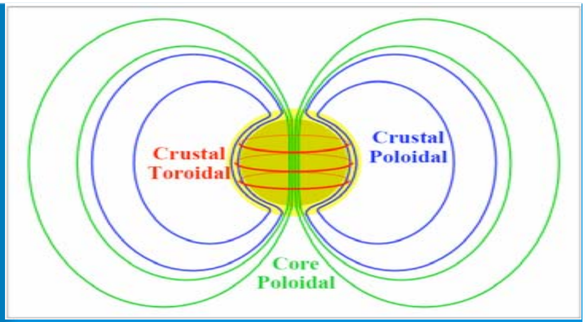

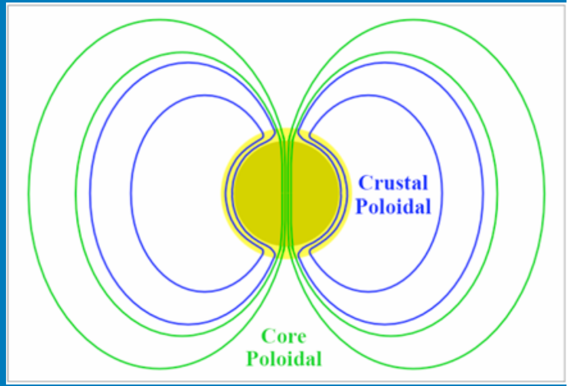

1. Proper modeling of magnetic field geometry is still missing
2. Are the QPOs related to crust oscillations?
3. Do we understand the spectrum?
   - Continuous or discrete?
   - Maybe a mixture?
4. Does the built-up stress, which ruptures the surface, excites any type of spheroidal modes (f-, s-, i-) ?
   - The accumulation of stress in the fluid core will create both density and velocity variations in the core!
   - Will such oscillations produce detectable GWs?

Numerical Codes

HRSC methods implemented in different numerical codes:

- Tonik: 2D polar, fixed spacetime (Font, Stegioulas, Kokkotas, 2001) (NS, Apostolatos, Font, 2004)
- Coconut: 2D polar, CFC approximation (Dimmelmeier, Font, Mueller) (Dimmelmeier, NS, Font, 2006)
- Cactus/Whisky: 3D Cartesian, full GR evolution (Baiotti, Hawke, Montero, Loeffler, Rezzolla, NS, Font, Seidel, 2004),
- Cactus/Pizza: 3D Cartesian, full GR evolution (W. Kastaun, 2006)

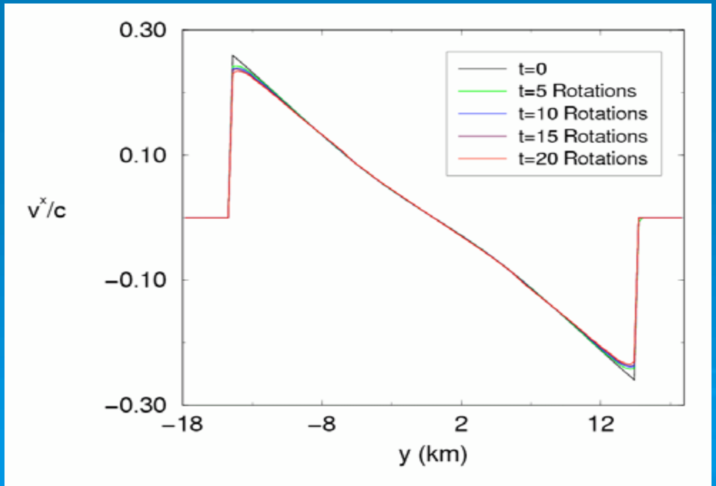

Initial Data: *imported RNS models* (Stergioulas, Friedman 1995).

Best numerical scheme:

3rd order PPM reconstruction

(Font, Stergioulas, Kokkotas 2001)

(NS, Font 2001)

Hydrodynamical Evolution

General-Relativistic Hydrodynamics:

$$\nabla_a T^{ab} = 0$$ Energy and momentum conservation

$$\nabla_a(\rho u^a) = 0$$ Baryon number conservation

1st-order hyperbolic form:

$$\partial_t \vec{U} + \partial_i \vec{F}^i = \vec{S}$$

$\vec{S}$	State vector	ρ	Rest-mass density
$\vec{F}^i$	Fluxes	e	Specific int. energy
$\vec{U}$	Sources	v^i	3-velocity

Primitive variables

$$D = \sqrt{\gamma} W \rho$$

$$\tau = \sqrt{\gamma}(\rho h W^2 - p - W\rho)$$

$$S_i = \sqrt{\gamma}\rho h W^2 v_i$$

Conserved variables

$$W = \alpha u^t$$

$$h = 1 + e + \frac{p}{\rho}$$

HRSC methods:

Solution of local Riemann problem in each cell:

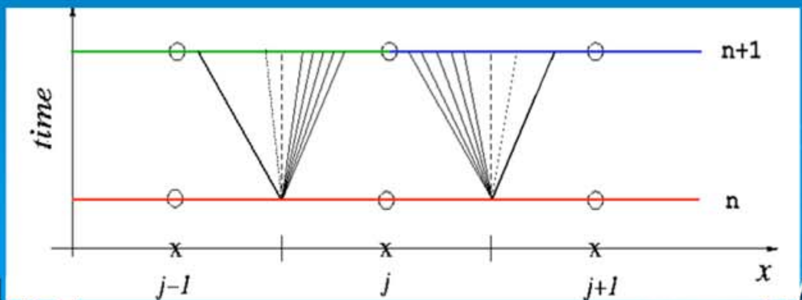

- Shock capturing without artificial viscosity
- High-order, oscillation-free reconstructions

Axisymmetric Modes
in Cowling Approximation

Axisymmetric modes for uniform or differential rotation with *fixed* spacetime evolution (Cowling approximation) :

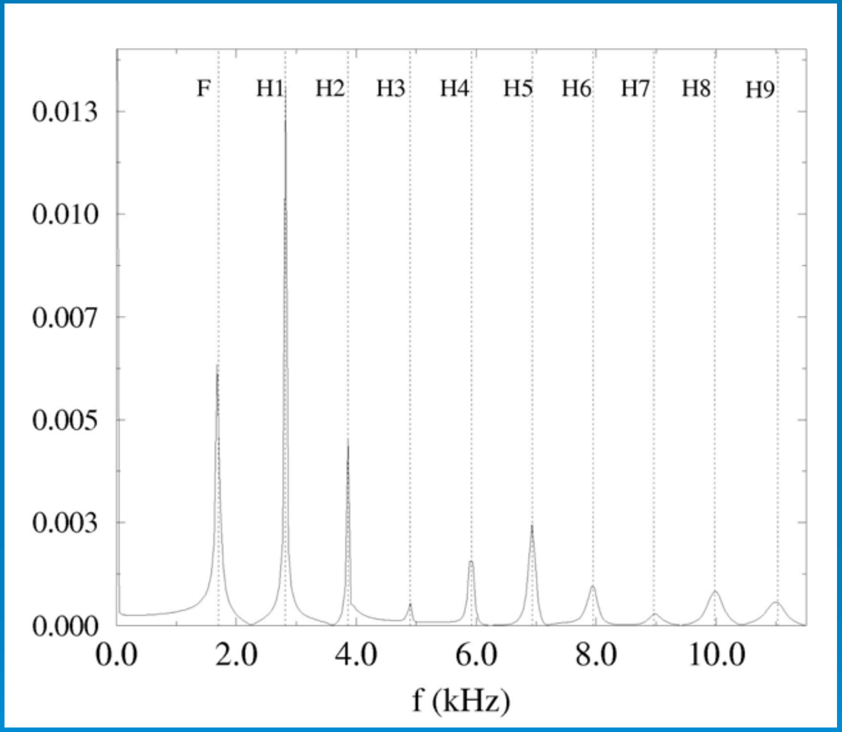

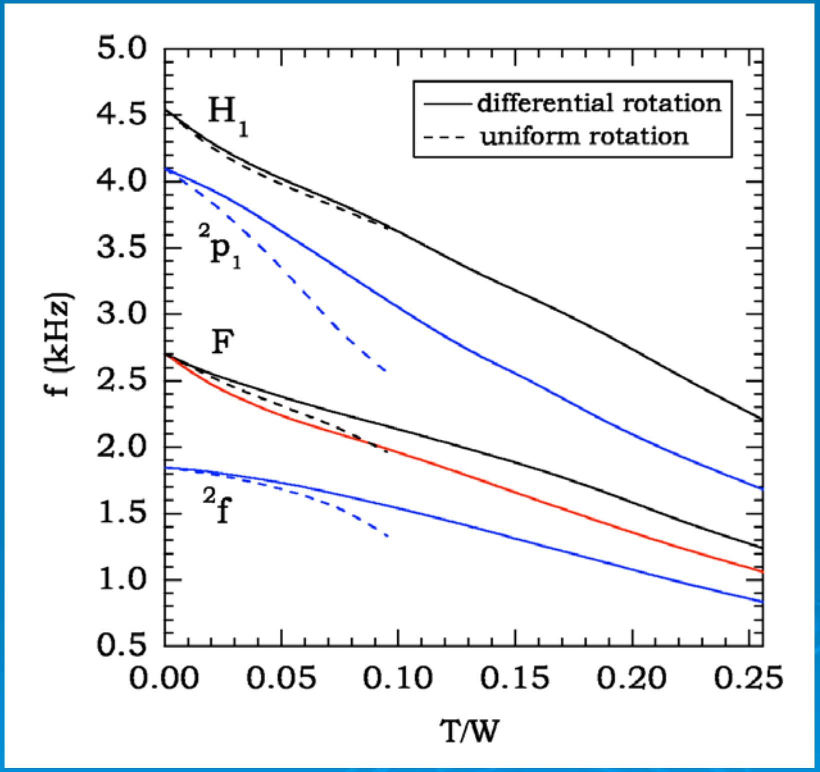

Font, Stergioulas, Kokkotas(2002)

Stergioulas, Apostolatos, Font (2004)

Axisymmetric Modes in CFC Approximation

Spacetime evolution with Spatially Conformally Flat Condition (CFC/IWM)

Sensitive to Differential Rotation

not sensitive to Differential Rotation

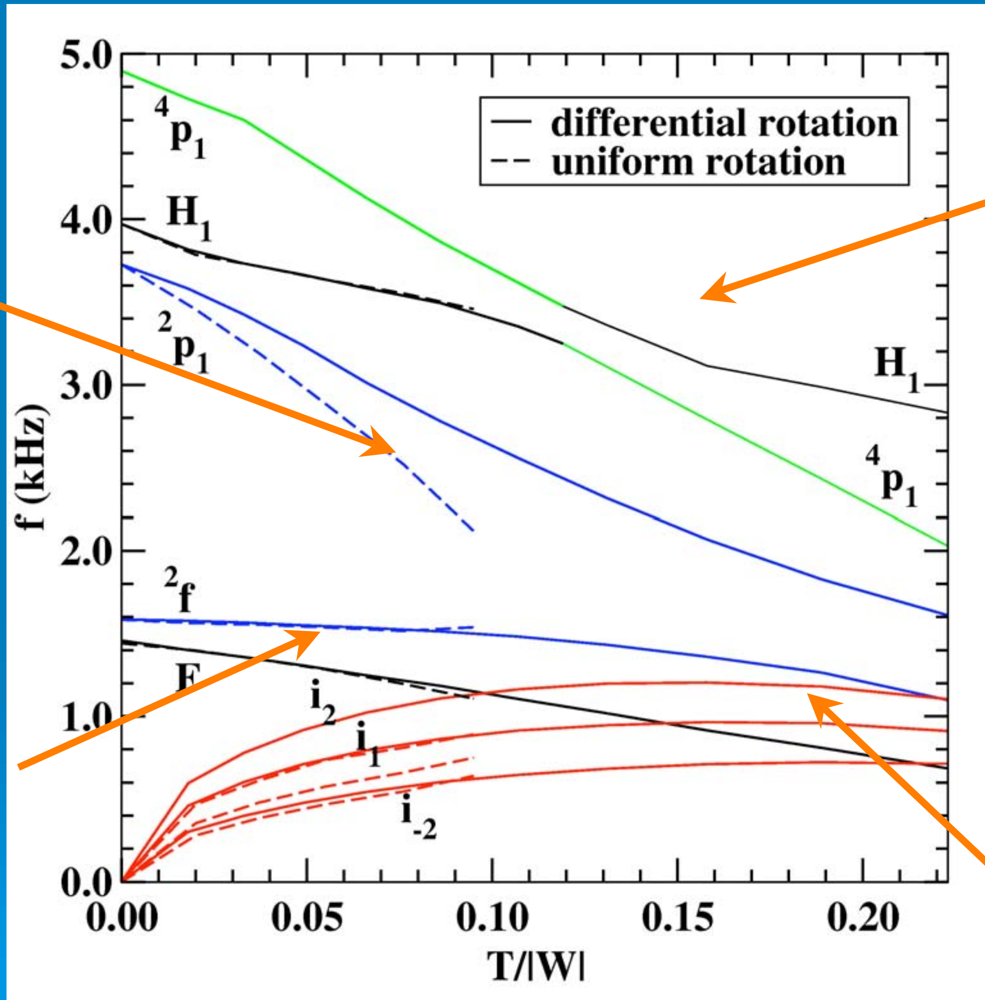

Avoided Crossing

Frequencies Shifted to 1-2 kHz range

Maximum frequency

Dimmelmeier, Stergioulas & Font (2005)

Gravitational Wave Emission

Characteristic signal amplitude for slowest rotating model ($T/|W|$~2%) at 10kpc (individually excited modes with 20ms integration time).

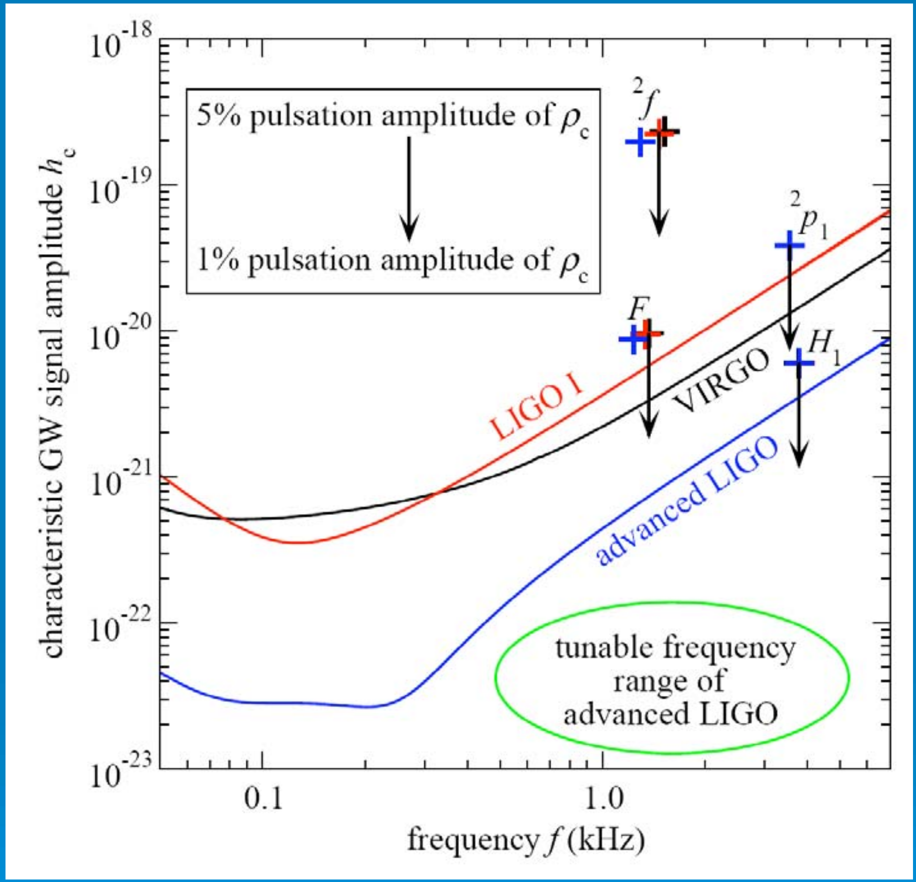

For GW-Asteroseismology, need advanced detectors with better sensitivity at several kHz.

GW Strain

Galactic source (10 kpc)

Multi-mode pulsational configuration with $\delta\varepsilon_c \sim$ 1-5 %

Collapse Simulations:

$\Delta t \sim$20 ms

$E_{GW} \sim 10^{-8} M_\odot$

Characteristic strain:

$$h_c(\nu) = \frac{\sqrt{2}}{\pi d}\sqrt{\frac{dE}{d\nu}}$$

Detector rms strain:

$$h_{rms}(\nu) \equiv \sqrt{S_h \nu}$$

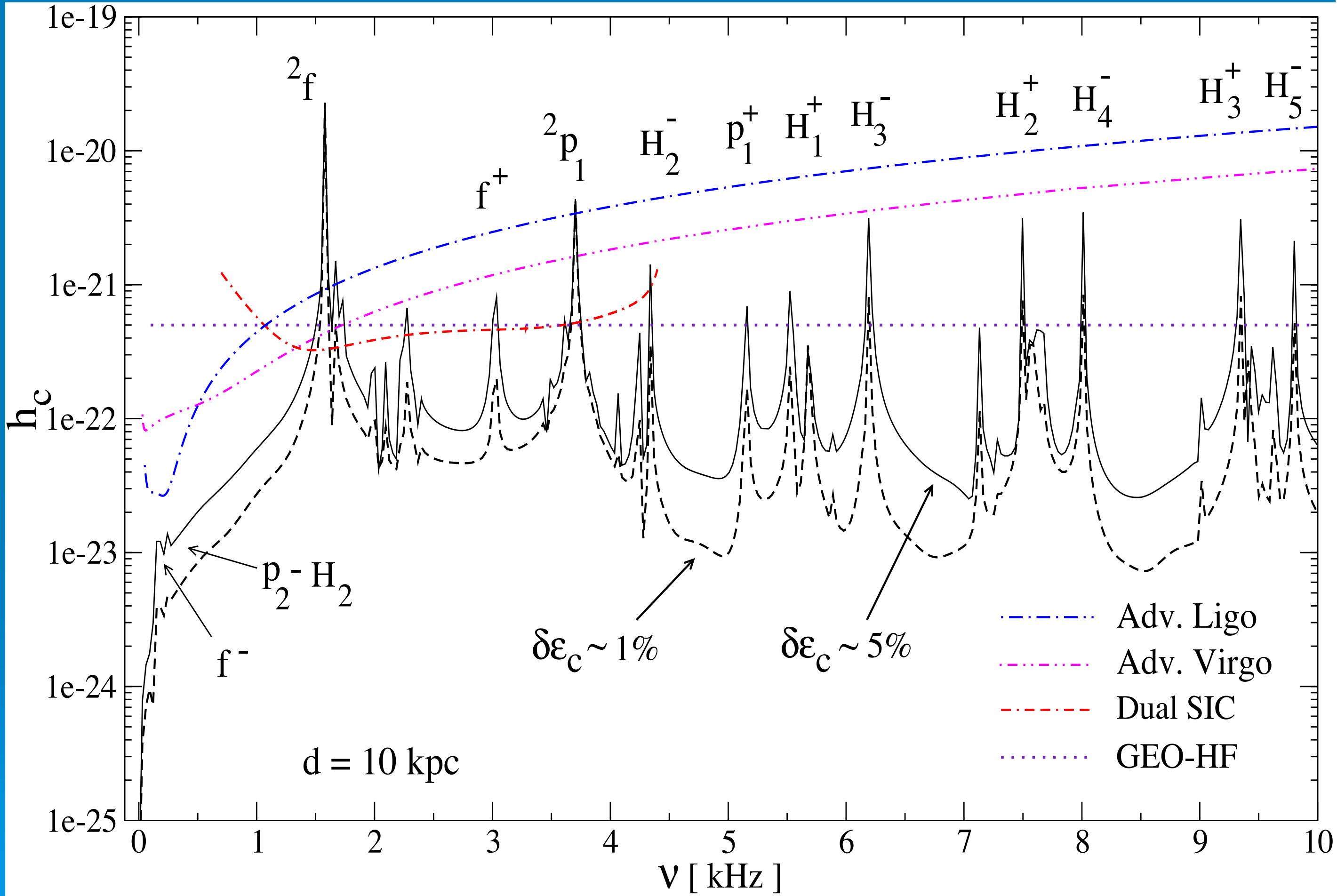

Where we are now :

- For a first time we observed NS oscillations ? (t-modes ?)
- f-modes: (unstable) good source of GWs
- r-modes: (unstable) good source only from LMXB
- w-modes: can be seen in core collapse to BH
- Non-linear numerical evolutions “overtook” perturbation methods in various parts of the study
- Complicated cases e.g. *dynamics of hot newly born fast (differential) rotating NS with complicated magnetic fields* are still to be studied.

…still long way to go!

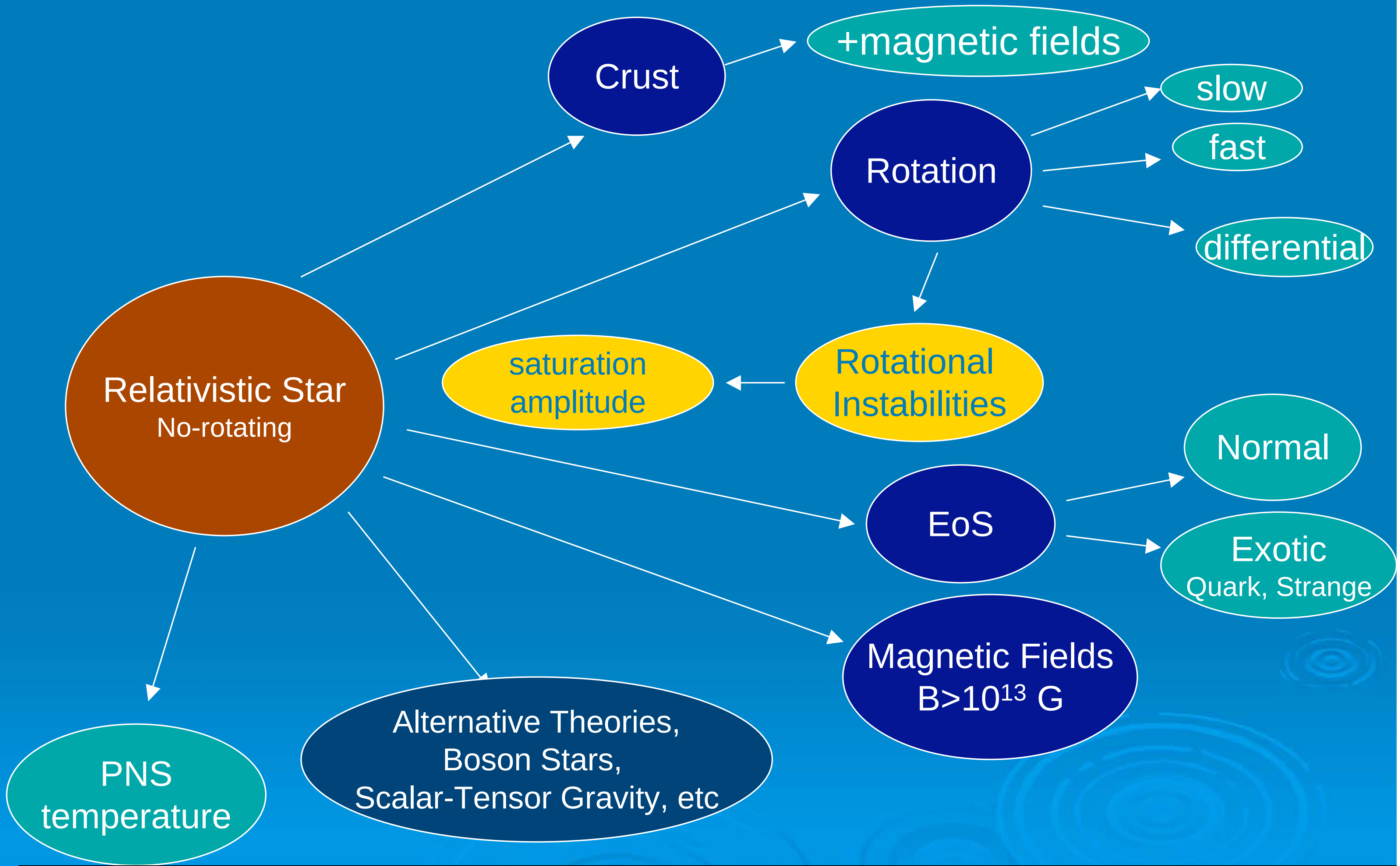

…needs synergism of perturbation theory and nonlinear numerical GR